

TLR9 and beclin 1 crosstalk regulates muscle AMPK activation in exercise

<https://doi.org/10.1038/s41586-020-1992-7>

Received: 7 September 2018

Accepted: 12 December 2019

Published online: 12 February 2020

 Check for updates

Yang Liu^{1,2}✉, Phong T. Nguyen^{1,2}, Xun Wang^{3,4}, Yuting Zhao¹, Corbin E. Meacham^{3,4}, Zhongju Zou^{1,2}, Bogdan Bordicanu^{3,4}, Manuel Johanns⁵, Didier Vertommen⁵, Tobias Wijshake¹, Herman May⁶, Guanghua Xiao⁷, Sanae Shoji-Kawata¹, Mark H. Rider⁵, Sean J. Morrison^{3,4}, Prashant Mishra^{3,4} & Beth Levine^{1,2,8}✉

The activation of adenosine monophosphate-activated protein kinase (AMPK) in skeletal muscle coordinates systemic metabolic responses to exercise¹. Autophagy—a lysosomal degradation pathway that maintains cellular homeostasis²—is upregulated during exercise, and a core autophagy protein, beclin 1, is required for AMPK activation in skeletal muscle³. Here we describe a role for the innate immune-sensing molecule Toll-like receptor 9 (TLR9)⁴, and its interaction with beclin 1, in exercise-induced activation of AMPK in skeletal muscle. Mice that lack TLR9 are deficient in both exercise-induced activation of AMPK and plasma membrane localization of the GLUT4 glucose transporter in skeletal muscle, but are not deficient in autophagy. TLR9 binds beclin 1, and this interaction is increased by energy stress (glucose starvation and endurance exercise) and decreased by a BCL2 mutation^{3,5} that blocks the disruption of BCL2–beclin 1 binding. TLR9 regulates the assembly of the endolysosomal phosphatidylinositol 3-kinase complex (PI3KC3-C2)—which contains beclin 1 and UVAG—in skeletal muscle during exercise, and knockout of beclin 1 or UVAG inhibits the cellular AMPK activation induced by glucose starvation. Moreover, TLR9 functions in a muscle-autonomous fashion in ex vivo contraction-induced AMPK activation, glucose uptake and beclin 1–UVAG complex assembly. These findings reveal a heretofore undescribed role for a Toll-like receptor in skeletal-muscle AMPK activation and glucose metabolism during exercise, as well as unexpected crosstalk between this innate immune sensor and autophagy proteins.

TLR9 senses unmethylated CpG DNA from bacteria and mitochondrial DNA (mtDNA) to initiate type I interferon and pro-inflammatory cytokine production in immune cells^{4,6}. Exogenously administered TLR9 ligands activate AMPK in cardiomyocytes and neurons and protect against hypoxic injury⁷. However, aside from studies in the heart^{8,9}, it is unknown whether TLR9 has a physiological role in nonimmune cells *in vivo*.

We performed a proteomic screen in HeLa cells to identify proteins that interact with a functionally important region of beclin 1, amino acids 267–284 (data not shown). This region of beclin 1—when linked to the cell-penetrating leader sequence Tat—is sufficient to induce autophagy and exert beneficial effects in animal models of human disease². The flexibility of this region is crucial for conformational changes that promote the membrane association and lipid kinase activity of beclin 1-containing class III phosphatidylinositol 3-kinase (PI3KC3) complexes¹⁰. We identified TLR7, an endosomal Toll-like receptor that recognizes single-strand RNA, as a high confidence interactor with this region of beclin 1. We confirmed that exogenously expressed TLR7, as

well as the related protein TLR9, co-immunoprecipitates with beclin 1 in HeLa cells (Extended Data Fig. 1a, b).

We explored whether there is a regulated interaction between beclin 1 and TLR9 during energy stress, including glucose starvation in cultured cells and endurance exercise in mice. We focused on TLR9 because mtDNA is sensed by endosomal TLR9 rather than TLR7⁹ and exercise induces mitophagy (autophagic degradation of mitochondria)¹¹, which may be an intracellular route for the delivery of mtDNA to the lumen of TLR9-containing endolysosomes¹². We confirmed that endogenous beclin 1 co-immunoprecipitates with TLR9 tagged with C-terminal haemagglutinin (HA) (TLR9–HA) in U2OS cells (Fig. 1a). Mutational analyses showed that deletion of amino acids 267–284 (the bait in our proteomic screen) from Flag epitope-tagged beclin 1 or deletion of the cytoplasmic Toll/interleukin-1 receptor (TIR) domain of TLR9–HA blocks binding between TLR9–HA and beclin 1 (Extended Data Fig. 1c, d). The interaction between beclin 1 and the TIR domain of TLR9 is direct (Extended Data Fig. 1e). Moreover, the binding of TLR9–HA and beclin 1 is upregulated by glucose starvation (a low-energy stress condition) but

¹Center for Autophagy Research, Department of Internal Medicine, University of Texas Southwestern Medical Center, Dallas, TX, USA. ²Howard Hughes Medical Institute, University of Texas Southwestern Medical Center, Dallas, TX, USA. ³Children's Medical Center Research Institute, University of Texas Southwestern Medical Center, Dallas, TX, USA. ⁴Department of Pediatrics, University of Texas Southwestern Medical Center, Dallas, TX, USA. ⁵De Duve Institute, Université Catholique de Louvain, Brussels, Belgium. ⁶Division of Cardiology, Department of Internal Medicine, University of Texas Southwestern Medical Center, Dallas, TX, USA. ⁷Department of Clinical Sciences, University of Texas Southwestern Medical Center, Dallas, TX, USA. ⁸Department of Microbiology, University of Texas Southwestern Medical Center, Dallas, TX, USA. [✉]e-mail: yang.liu3@utsouthwestern.edu; beth.levine@utsouthwestern.edu

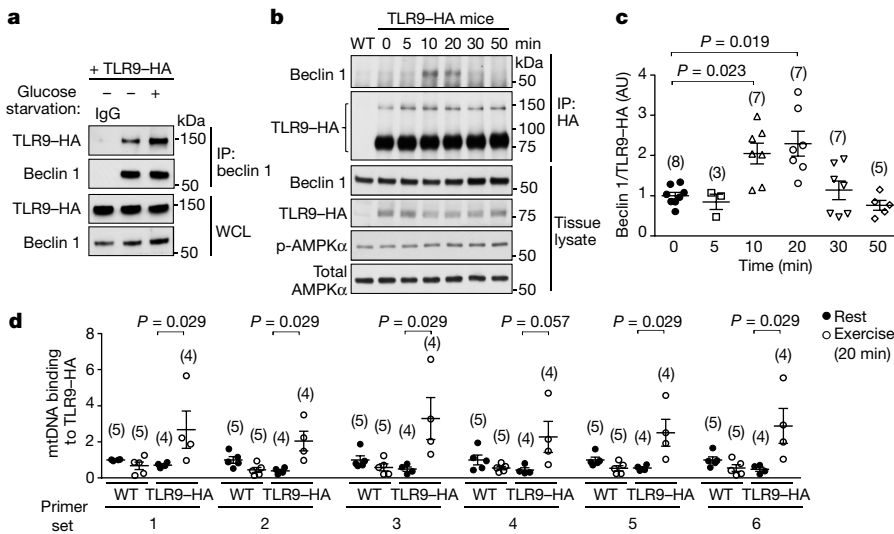


Fig. 1 | TLR9 interacts with beclin 1 during glucose starvation and exercise.

a, Co-immunoprecipitation (IP) of transfected TLR9–HA with endogenous beclin 1 in U2OS cells cultured in normal or glucose-starvation medium (1 h). Results representative of three independent experiments. **b, c**, Representative western blots (**b**) and quantification (**c**) of beclin 1 co-immunoprecipitated with TLR9–HA in vastus lateralis muscles from TLR9–HA mice at indicated duration of exercise. Extended Data Fig. 2b provides quantification of p-AMPK α (T172)/total AMPK α . Data are mean \pm s.e.m. Unpaired two-tailed *t*-test with Hommel method. Values at 0 min are considered as 1, results are expressed as relative

arbitrary units (AU) and are combined data from 3 independent experiments. Similar results were observed in each experiment. WT, wild type.

d, Quantification of mtDNA co-immunoprecipitated with TLR9–HA from gastrocnemius muscles of wild-type and TLR9–HA mice (Methods). For each mtDNA primer set, the value of wild-type mice at rest is considered to be 1. Data are mean \pm s.e.m. Two-tailed Mann–Whitney test. For **c, d**, data points are individual mice (sample size indicated in parentheses). WCL, whole-cell lysate. For uncropped gels, see Supplementary Fig. 1.

not by other stressors, such as amino acid starvation or mitochondrial damaging agents (Fig. 1a, Extended Data Fig. 1f, g).

Next, we determined whether beclin 1 interacts with TLR9 in skeletal muscle during exercise. We confirmed that *Tlr9* mRNA is expressed in mouse skeletal muscle at levels similar to those in other nonimmune organs (Extended Data Fig. 1h). Additionally, *Tlr9* mRNA expression is undetectable in embryonic myoblasts, but markedly increases after differentiation into myotubes (Extended Data Fig. 1i). Given the well-established difficulty in generating antibodies that reliably detect endogenous TLR9, we used CRISPR technology to construct knock-in mice with an HA epitope tag inserted at the C terminus of the *Tlr9* locus (*Tlr9*–HA knock-in mice; hereafter referred to as TLR9–HA mice) (Extended Data Fig. 1j, k). These mice express TLR9–HA in all the tissues we examined (Extended Data Fig. 1l, m). The predominant form is the active approximately 80-kDa cleavage product that consists of a carboxyl-terminal fragment containing a portion of the TLR9 ectodomain, the transmembrane domain and the cytoplasmic domain¹³. This form is generated by endolysosomal proteolysis, and mediates ligand recognition and subsequent signalling cascades^{4,14}.

Endogenous beclin 1 in skeletal muscle co-immunoprecipitated with TLR9–HA in a time-dependent manner after the initiation of treadmill exercise. The interaction was first detected at 10 min, plateaued at 20 min and was undetectable by 50 min (Fig. 1b, c, Extended Data Fig. 2a). The interaction of beclin 1 and TLR9 at 10 min corresponded to the first time point at which increased AMPK phosphorylation in skeletal muscle was detected (Fig. 1b, Extended Data Fig. 2b). In spleen (the tissue with highest expression of TLR9), exercise did not increase beclin 1–TLR9 interaction or AMPK phosphorylation (Extended Data Fig. 2c–f). Moreover, at 20 min after exercise (but not at rest), mtDNA—but not genomic DNA—co-immunoprecipitated with TLR9–HA in muscle (Fig. 1d, Extended Data Fig. 3a). Up to 90 min after exercise, no increase in circulating mtDNA was detectable (Extended Data Fig. 3b), which suggests that mtDNA may be delivered to endolysosomal TLR9 during exercise via an intracellular route. ODN2395, an exogenous TLR9 ligand, did not increase AMPK phosphorylation in mouse muscle explants (Extended Data Fig. 3c–e). Thus, in skeletal muscle during

acute exercise, beclin 1 and TLR9 interact and—simultaneously—an endogenous ligand (mtDNA) associates with the innate immune sensor TLR9. We cannot exclude the possibility that additional CpG DNA ligands associate with TLR9 in muscles during exercise.

In view of previously established links between beclin 1 and exercise-induced activation of AMPK in muscles³, these findings suggested that TLR9 might exert metabolic functions in muscle tissue during exercise. Therefore, we studied the skeletal muscles of *Tlr9*^{−/−} mice¹⁵ during treadmill exercise. Fibre type, mitochondrial respiratory capacity, and capillary density were similar in muscles of wild-type and *Tlr9*^{−/−} mice (Extended Data Fig. 4a–g). Cardiac function was also similar in *Tlr9*^{−/−} and wild-type mice (Extended Data Fig. 4h). However, compared to littermate controls, *Tlr9*^{−/−} mice were deficient in exercise-induced activation of AMPK in muscles, as determined by the quantification of phosphorylation of AMPK and its downstream targets (TBC1D1, acetyl-CoA carboxylase (ACC) and raptor) (Fig. 2a, b, Extended Data Fig. 5a–d). Consistent with defective AMPK and TBC1D1 phosphorylation, *Tlr9*^{−/−} mice did not exhibit exercise-induced localization of the GLUT4 glucose transporter to the plasma membrane (Fig. 2c, d, Extended Data Fig. 5e–h), which is essential for exercise-stimulated glucose uptake in muscles¹⁶. Furthermore, *Tlr9*^{−/−} mice did not display decreased plasma glucose levels during exercise (Fig. 2e), and they exhibited decreased exercise endurance (Extended Data Fig. 5i).

Muscles of *Tlr9*^{−/−} and wild-type mice were similar with respect to known regulators of AMPK activation in response to exercise, including increased AMP/ATP and ADP/ATP ratios, decreased glycogen levels, and levels of total LKB1 and LKB1 phosphorylated at serine 428¹⁷ (Extended Data Fig. 6a–h). Moreover, downstream glucose-transport pathways regulated by AMPK were intact in *Tlr9*^{−/−} mice, as administration of a direct AMPK activator (PF-739¹⁸) to *Tlr9*^{−/−} and wild-type mice resulted in similar levels of TBC1D1 phosphorylation in skeletal muscle and a similar decline in blood glucose levels (Extended Data Fig. 6i–k). Thus, TLR9 is required for AMPK activation in skeletal muscles and AMPK-regulated effects on glucose metabolism during exercise through a newly defined mechanism.

To evaluate whether TLR9 in haematopoietic cells contributes to exercise-induced activation of AMPK in skeletal muscles, we

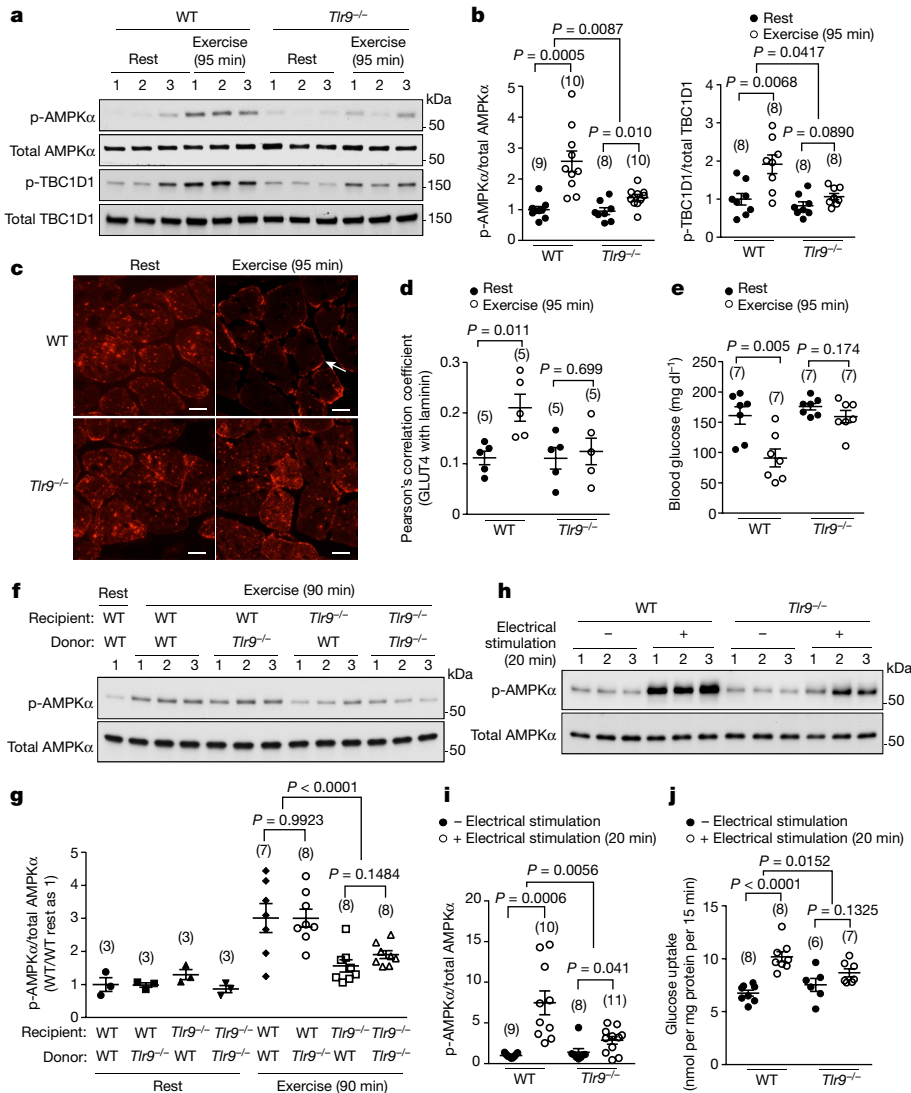


Fig. 2 | TLR9 is required for exercise-induced activation of AMPK in muscles. **a, b.** Representative western blots (**a**) and quantification (**b**) of p-AMPK(T172) and p-TBC1D1(S237) in vastus lateralis muscles from wild-type and *Tlr9*^{-/-} mice. **c, d.** Representative images of GLUT4 staining in vastus lateralis muscles (**c**), and quantification (**d**) of colocalization of GLUT4 and laminin in extensor digitorum longus (EDL) muscles from wild-type and *Tlr9*^{-/-} mice. Extended Data Fig. 5g shows representative images of EDL muscles. At least 100 muscle fibres were analysed per mouse. Arrow, GLUT4 localization at plasma membrane. Scale bars, 20 µm. **e.** Blood glucose levels. **f, g.** Representative western blots (**f**) and quantification (**g**) of AMPK phosphorylation in vastus lateralis muscles from indicated recipient mice transplanted with indicated donor bone marrow. **h, i.** Representative western blots (**h**) and quantification (**i**) of AMPK

noncompetitively transplanted irradiated wild-type or *Tlr9*^{-/-} recipient mice with bone marrow cells from either wild-type or *Tlr9*^{-/-} donor mice. Recipient mice exhibited high levels of donor-cell chimerism in the peripheral blood (Extended Data Fig. 7a, b). A greater increase in exercise-induced phosphorylation of AMPK and its substrate TBC1D1 in skeletal muscles was observed in wild-type compared to *Tlr9*^{-/-} recipient mice (Fig. 2f, g, Extended Data Fig. 7c, d). Notably, donor genotype had no effect on AMPK or TBC1D1 phosphorylation in either recipient genotype, which indicates that TLR9 in haematopoietic cells is not required for the TLR9-dependent activation of AMPK in skeletal muscles that is induced by exercise.

To further assess whether TLR9 functions in a tissue-autonomous manner in AMPK activation in skeletal muscles, we performed ex vivo electrical stimulation to induce muscle contraction.

phosphorylation in ex vivo EDL muscles from wild-type and *Tlr9*^{-/-} mice. **j.** Glucose uptake in ex vivo EDL muscles. Western blots and images are from one representative experiment, and quantification data are combined from three independent experiments. Similar results were observed for each experiment. In **b, d, e, g, i, j**, data points are individual mice (**b, d, e, g**) or muscles (**i, j**); sample size is indicated in parentheses. Data are mean \pm s.e.m. In **b, d, e, i, j**, unpaired two-tailed *t*-test to compare different conditions per genotype. Two-way analysis of variance (ANOVA) for the magnitude of changes between different conditions in mice of different genotypes. In **g**, unpaired two-tailed *t*-test for differences between donor genotypes for each recipient genotype and two-way ANOVA for differences between recipient genotypes. For uncropped gels, see Supplementary Fig. 1.

Similar to observations during treadmill exercise, muscles from wild-type (as compared to *Tlr9*^{-/-}) mice displayed a greater increase in ex vivo contraction-induced phosphorylation of AMPK and TBC1D1 (Fig. 2h, i, Extended Data Fig. 7e, f). Importantly, there was a corresponding decrease in ex vivo contraction-stimulated glucose uptake in muscles of *Tlr9*^{-/-} mice (Fig. 2j). Therefore, TLR9 functions in a muscle-cell-autonomous manner to regulate AMPK activation and glucose metabolism. This may contribute to alterations in muscle AMPK activation, serum glucose levels and exercise endurance in *Tlr9*^{-/-} mice, although additional physiological factors may also influence these phenotypes *in vivo*.

The defects in exercise-induced activation of AMPK and plasma membrane GLUT4 localization in skeletal muscle, as well as in exercise endurance, in *Tlr9*^{-/-} mice closely resembled phenotypes that have

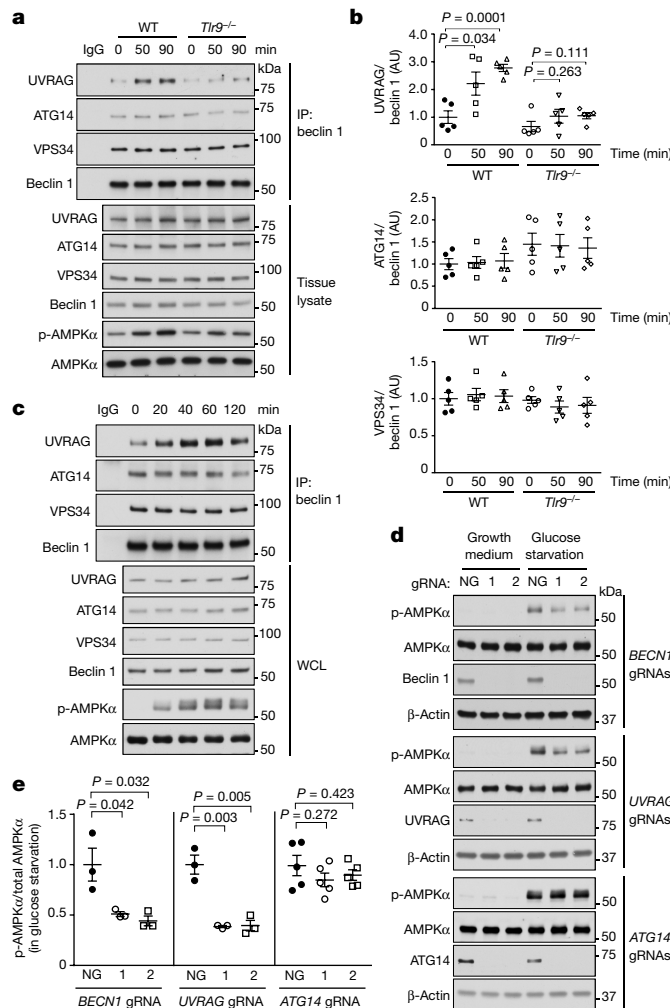


Fig. 3 | TLR9 is required for the beclin 1–UVRAG interaction during exercise.

a, Co-immunoprecipitation of UVRAG, ATG14 or VPS34 with beclin 1 in tibialis anterior muscles from wild-type and *Tlr9^{-/-}* mice at indicated duration of exercise. Tissue lysate from the wild-type 0-min sample was used for control IgG precipitation. **b**, Quantification of co-immunoprecipitation of UVRAG, ATG14 and VPS34 with beclin 1 in three independent experiments using design shown in **a**. Data points are individual mice ($n=5$). Data are mean \pm s.e.m. Unpaired two-tailed *t*-test comparing 50-min or 90-min exercise versus 0-min condition for each genotype. **c**, Co-immunoprecipitation of UVRAG, ATG14 or VPS34 with beclin 1 in U2OS cells at indicated time points after glucose starvation. Similar results were observed in three independent experiments. **d, e**, Representative blots (**d**) and quantification (**e**) of effects of indicated gene knockout on AMPK activation in U2OS cells cultured in normal or glucose starvation medium (1 h). Two independent guide RNAs (gRNAs) per gene target. Quantification data from three (BECN1 gRNAs and UVRAG gRNAs) or five (ATG14 gRNAs) independent experiments. Data are mean \pm s.e.m. Unpaired two-tailed *t*-test. NG, no gRNA. For uncropped gels, see Supplementary Fig. 1.

previously been reported³ in *Becn1^{+/−}* mice and genetically engineered mice that express a mutant BCL2 protein that cannot be phosphorylated (BCL2(T69A/S70A/S87A), hereafter termed BCL2 AAA) and that prevents exercise-induced disruption of BCL2–beclin 1 binding. However, unlike *Becn1^{+/−}* mice or BCL2 AAA mice, *Tlr9^{-/-}* mice did not exhibit defects in exercise-induced autophagic flux in skeletal muscles (Extended Data Fig. 8a, b). Thus, impaired exercise-induced autophagy may not be responsible for defects in AMPK activation in *Becn1^{+/−}* or BCL2 AAA mice; instead, the functions of beclin 1 in autophagy and AMPK activation may be independent.

We hypothesized that the defect in AMPK activation in BCL2 AAA mice³ may involve decreased interaction of beclin 1 with TLR9.

We crossed BCL2 AAA mice with TLR9–HA mice. The exercise-induced increase in the interaction between beclin 1 and TLR9–HA observed in wild-type mice was not observed in BCL2 AAA mice (Extended Data Fig. 8c, d). Similarly, in cultured cells that stably express BCL2 AAA¹⁹, glucose starvation did not increase the binding of beclin 1 to TLR9–HA (Extended Data Fig. 8e–g). Thus, the constitutive binding of beclin 1 by BCL2 blocks not only stress-induced autophagy^{3,5}, but also the interaction of beclin 1 and TLR9 induced by glucose starvation or exercise.

To explore the mechanism by which the TLR9–beclin 1 interaction regulates AMPK activation, we evaluated the effect of TLR9 knockout on the association of beclin 1 with other members of PI3KC3 complexes in skeletal muscle during exercise. The two main complexes are PI3KC3-C1 (which contains beclin 1, VPS34, VPS15 and ATG14, and functions in autophagic vesicle nucleation) and PI3KC3-C2 (which contains beclin 1, VPS34, VPS15 and UVAG, and functions in endolysosomal and autophagolysosomal maturation)²⁰. During exercise, increased UVRAG—but not increased ATG14—bound to beclin 1, suggesting enhanced assembly of PI3KC3-C2 (Fig. 3a, b, Extended Data Fig. 9a, b). This increased UVRAG–beclin 1 interaction was blocked in *Tlr9^{-/-}* mice (Fig. 3a, b). Moreover, increased UVRAG–beclin 1 binding occurred during ex vivo, electrical-stimulation-induced contraction in muscles from wild-type, but not *Tlr9^{-/-}*, mice (Extended Data Fig. 9c, d). Additionally, glucose starvation in U2OS cells led to a steady increase in UVRAG–beclin 1, but not ATG14–beclin 1, interaction (Fig. 3c). CRISPR-mediated knockout of beclin 1 and UVRAG—but not of ATG14—reduced AMPK phosphorylation induced by glucose starvation (Fig. 3d, e) without affecting total levels of LKB1 or LKB1 Ser428 phosphorylation (Extended Data Fig. 10). Thus, the PI3KC3-C2 complex may regulate AMPK activity.

Our data are consistent with a model in which crosstalk between TLR9 and the PI3KC3-C2 complex containing beclin 1 and UVRAG leads to AMPK activation during energy stress. Our findings integrate three disparate aspects of cell biology—innate immune sensing, protein complexes containing autophagy proteins, and AMPK activation—in the responses of skeletal muscle to exercise. A previous study²¹ in immune cells indicated that autophagy proteins involved in LC3-associated phagocytosis regulate TLR9 responses to DNA immune complexes. The link between an innate immune receptor capable of recognizing mtDNA and the activation of AMPK may serve as a fundamental mechanism to maintain muscle homeostasis during exercise. The autophagy machinery is an ancient and highly conserved set of proteins that mediates responses to nutritional stress even in unicellular organisms. Teleologically, these proteins may also have evolved to respond to stresses unique to metazoan organisms such as exercise—a process that requires increased metabolic resources, especially in skeletal muscle. The crosstalk between an innate immune sensor that responds to DNA and between autophagy proteins during exercise may represent a more general paradigm in which innate immune sensors of danger and cellular quality-control mechanisms intersect to maintain normal mammalian physiology.

Online content

Any methods, additional references, Nature Research reporting summaries, source data, extended data, supplementary information, acknowledgements, peer review information; details of author contributions and competing interests; and statements of data and code availability are available at <https://doi.org/10.1038/s41586-020-1992-7>.

- Kjøbsted, R. et al. AMPK in skeletal muscle function and metabolism. *FASEB J.* **32**, 1741–1777 (2018).
- Levine, B. & Kroemer, G. Biological functions of autophagy genes: a disease perspective. *Cell* **176**, 11–42 (2019).
- He, C. et al. Exercise-induced BCL2-regulated autophagy is required for muscle glucose homeostasis. *Nature* **481**, 511–515 (2012).
- Pandey, S., Kawai, T. & Akira, S. Microbial sensing by Toll-like receptors and intracellular nucleic acid sensors. *Cold Spring Harb. Perspect. Biol.* **7**, a016246 (2015).

5. Wei, Y., Pattingre, S., Sinha, S., Bassik, M. & Levine, B. JNK1-mediated phosphorylation of Bcl-2 regulates starvation-induced autophagy. *Mol. Cell* **30**, 678–688 (2008).
6. West, A. P. & Shadel, G. S. Mitochondrial DNA in innate immune responses and inflammatory pathology. *Nat. Rev. Immunol.* **17**, 363–375 (2017).
7. Shintani, Y. et al. TLR9 mediates cellular protection by modulating energy metabolism in cardiomyocytes and neurons. *Proc. Natl Acad. Sci. USA* **110**, 5109–5114 (2013).
8. Zhou, D. C. et al. CpG oligodeoxynucleotide preconditioning improves cardiac function after myocardial infarction via modulation of energy metabolism and angiogenesis. *J. Cell. Physiol.* **233**, 4245–4257 (2018).
9. Omiya, S. et al. Toll-like receptor 9 prevents cardiac rupture after myocardial infarction in mice independently of inflammation. *Am. J. Physiol. Heart Circ. Physiol.* **311**, H1485–H1497 (2016).
10. Rostislavleva, K. et al. Structure and flexibility of the endosomal Vps34 complex reveals the basis of its function on membranes. *Science* **350**, aac7365 (2015).
11. Guan, Y., Drake, J. C. & Yan, Z. Exercise-induced mitophagy in skeletal muscle and heart. *Exerc. Sport Sci. Rev.* **47**, 151–156 (2019).
12. De Leo, M. G. et al. Autophagosome-lysosome fusion triggers a lysosomal response mediated by TLR9 and controlled by OCRL. *Nat. Cell Biol.* **18**, 839–850 (2016).
13. Ewald, S. E. et al. The ectodomain of Toll-like receptor 9 is cleaved to generate a functional receptor. *Nature* **456**, 658–662 (2008).
14. Majer, O. et al. Release from UNC93B1 reinforces the compartmentalized activation of select TLRs. *Nature* **575**, 371–374 (2019).
15. Hemmi, H. et al. A Toll-like receptor recognizes bacterial DNA. *Nature* **408**, 740–745 (2000).
16. Zisman, A. et al. Targeted disruption of the glucose transporter 4 selectively in muscle causes insulin resistance and glucose intolerance. *Nat. Med.* **6**, 924–928 (2000).
17. Xie, Z., Dong, Y., Scholz, R., Neumann, D. & Zou, M. H. Phosphorylation of LKB1 at serine 428 by protein kinase C- ζ is required for metformin-enhanced activation of the AMP-activated protein kinase in endothelial cells. *Circulation* **117**, 952–962 (2008).
18. Cokorinos, E.C. et al. Activation of skeletal muscle AMPK promotes glucose disposal and glucose lowering in non-human primates and mice. *Cell Metab.* **25**, 1147–1159 (2017).
19. Wei, Y. et al. The stress-responsive kinases MAPKAPK2/MAPKAPK3 activate starvation-induced autophagy through Beclin 1 phosphorylation. *eLife* **4**, e05289 (2015).
20. Hurley, J. H. & Young, L. N. Mechanisms of autophagy initiation. *Annu. Rev. Biochem.* **86**, 225–244 (2017).
21. Henault, J. et al. Noncanonical autophagy is required for type I interferon secretion in response to DNA-immune complexes. *Immunity* **37**, 986–997 (2012).

Publisher's note Springer Nature remains neutral with regard to jurisdictional claims in published maps and institutional affiliations.

© The Author(s), under exclusive licence to Springer Nature Limited 2020

Article

Methods

No statistical methods were used to predetermine sample size. For animal experiments, mice of the same genotype were randomly assigned to different treatment groups. Investigators were blinded to mouse genotype when measuring exercise endurance, acquiring images for autophagy analysis, and determining the fibre types and capillary density in muscles.

Mouse strains

All mice were housed in a pathogen-free facility under 12-h light–dark cycles with ad libitum access to food and water. All mouse experimental procedures were approved by the Institutional Animal Care and Use Committee at UT Southwestern Medical Center and performed in accordance with institutional guidelines. Eight- to twelve-week-old male mice were used, except for bone marrow transplantation experiments (see ‘Bone marrow transplantation’). *Tlr9*^{-/-} mice¹⁵, BCL2 AAA mice³ and GFP-LC3 transgenic mice²² have previously been described, and all strains were rederived in the UTSW Transgenic Mouse facility on a C57BL/6J background and further backcrossed to C57BL/6J for at least ten generations.

Tlr9-HA knock-in mice (termed TLR9–HA mice) were generated by CRISPR genome-editing technology at the Transgenic Core Facility at UT Southwestern Medical Center. gRNAs (targeting the *Tlr9* genome near the region that encodes the stop codon) and the donor oligonucleotide were designed, synthesized and validated by Sigma-Aldrich. The gRNA (antisense) targeted genome sequence is 5'-GGGACCTACAGCAGAACATAG-3'. The sequence of the donor oligonucleotide is 5'-TTCTGGGCCAGCTGAGTACAGCCCTGAC TAGGGACAACCGCCACTTCTATAACCAGAACTTCTGCAGGGACCTA CAGCAGAAATCCCATAAGCTGATGTTCCAGATTACGCTTAGCTCAGAGCAA CAGCTGGAAACAGCTGCATCTCATGTCTGGTCCCGAGATTGCTCT GCCTGCCTG-3'. After homologous recombination, the antisense protospacer-adjacent motif (PAM) sequence (CCG) recognition by Cas9 is diminished with a change of C to A (CAG), and this change also generates a PstI restriction site (CTGCAG) for further genotyping purposes. Genotyping primers were designed to generate a 473-bp PCR product for the wild-type allele (and a 500-bp PCR product for the knock-in allele) surrounding the targeting region. The PAM sequence is located 224 bp from the 5' end for both the wild-type and knock-in allele, and 246 bp and 273 bp from the 3' end for the wild-type and knock-in allele, respectively. The PCR products were subjected to PstI digestion. The knock-in allele PCR product is cut into two fragments (226 bp and 278 bp) and the wild-type allele PCR product is not cleaved. The sequences of genotyping primers are: forward, 5'-CTGCTGGCTCAGCAGCG-3' and reverse, 5'-GAACCTCCAGTCCTGTTCTGTG-3'.

To generate TLR9–HA mice, C57BL/6J (Jackson Laboratories) mouse zygotes were injected with gRNA, Cas9 mRNA and donor oligonucleotide into the pronucleus and cytoplasm, and then transferred to surrogate mothers for gestation. Genomic DNA isolated from tail biopsies of F₀ founders was used as a template for PCR genotyping. PCR products from each mouse were ligated into TA cloning vectors (Invitrogen) followed by bacterial transformation. Four colonies were selected for each mouse, and plasmids were purified and sequenced. An F₀ mouse with at least one plasmid carrying the correct knock-in sequence was considered as a positive founder. Because F₀ founders are mosaic, positive founders were bred with wild-type C57BL/6J mice (Jackson Laboratory) to isolate the knock-in allele. Mice from the F₁ generation that carried the knock-in allele were considered to have stable germline transmission, and were used for further breeding to generate homozygous knock-in mice for experiments.

Plasmids

pBICEP vectors encoding Flag-tagged full-length beclin 1 or deletion mutants were generated as previously described²³. cDNA encoding

full-length TLR9 or TLR9 amino acids 1–868 were cloned into pCR3.1 and a sequence encoding an HA tag was added to the C terminus of the *TLR9* cDNA. Codon-optimized *TLR7*cDNA²⁴ (a gift from G. Barton) was cloned into pCR3.1 with an HA tag sequence added to the C terminus. A lentivirus vector pXPR_023 expressing Cas9 and gRNA (a gift from J. Doench) was used for CRISPR-mediated gene knockout. The gRNAs targeting individual genes were designed using the Broad Institute Genetic Perturbation Platform (GPP) and the cloning of gRNAs into the pXPR_023 vector was performed according to the online instructions at the GPP web portal (<https://portals.broadinstitute.org/gpp/public/>). gRNA sequences used in the study for human genes are: *BECNI*, no. 1, 5'-GAACCTCAGCCGAAGACTGA-3' (sense); *BECNI*, no. 2, 5'-GAACGTT GCATTAAGACGT-3' (antisense); *UVRAG*, no. 1, 5'-AGGAATCCCTAAAT GAGCTG-3' (sense); *UVRAG*, no. 2, 5'-GAGTCTGTTAATTGACAC-3' (antisense); and *ATG14*, no. 1, 5'-TTGTTAGGGAGGCTAATCCA-3' (antisense); *ATG14*, no. 2, 5'-AGGAAGTAAAGACGGGTGTG-3' (sense).

Cell culture

HeLa, U2OS and Phoenix cell lines were obtained from and pre-authenticated by ATCC and used at low passage (<7) number. HeLa cells were additionally authenticated by the ATCC Cell Line Authentication Service using STR analysis. All cell lines were tested negative for mycoplasma contamination by PCR analysis at biweekly intervals throughout the study. Cells were cultured in DMEM (Gibco) containing 10% FBS (Gibco), 2 mM L-glutamine (Gibco) and non-essential amino acids (Gibco). Cells were transfected with lipofectamine 2000 (Invitrogen) according to the manufacturer's instructions. Glucose starvation was performed by replacing the normal growth medium with DMEM (without glucose) (Gibco) containing 10% dialysed FBS (Gibco) for the indicated time period. Amino acid starvation was performed by replacing the normal growth medium with Earle's Balanced Salt Solution (Gibco). For treatment with mitochondrial damaging agents and PF-739, cells cultured in normal growth medium were incubated with oligomycin (2.5 μM) and antimycin A (250 nM), carbonyl cyanide 3-chlorophenylhydrazone (CCCP) (5 μM) or PF-739 (5 μM) for 1 h. Lentiviruses carrying *Cas9*cDNA and gRNA for infection of U2OS cells to knock out targeted genes were packaged in Phoenix cells (ATCC) by cotransfection of pXPR_023 vector with packaging plasmids. Media containing virus particles were collected 48 h after transfection and used to infect U2OS cells for 3 h in the presence of 8 μg/ml polybrene. Seventy-two hours after infection, puromycin antibiotic selection was added to the medium of infected cells and maintained for four days before cells were used for experiments.

Lysate preparation and immunoprecipitation assays

Cells were lysed in lysis buffer containing 50 mM Hepes pH 7.4, 50 mM KCl, 50 mM NaF, 5 mM Na₂P₂O₇, 5 mM β-glycerophosphate, 1 mM EDTA, 1 mM EGTA, 1 mM Na₃VO₄, 1 mM dithiothreitol (DTT) supplemented with protease inhibitor cocktail (Roche) and 1% (v/v) Triton X-100. Lysates were precleared with protein A agarose (Sigma) for 1 h followed by immunoprecipitation of the indicated protein. For immunoprecipitation of Flag-beclin 1 or Myc-BCL2, anti-Flag-M2 agarose (Sigma) or anti-Myc agarose (Santa Cruz) was added to the lysate for 3 h. For immunoprecipitation of overexpressed TLR7–HA, TLR9–HA or endogenous beclin 1, anti-HA high-affinity antibody (11867423001, Roche) or anti-beclin 1 antibody (sc48341, Santa Cruz) was added to the pre-cleared lysate for 3 h before protein G agarose (Santa Cruz, for anti-HA high-affinity antibody) or protein A agarose (Sigma, for anti-beclin 1 antibody) was added for another 1.5 h. Immunoprecipitates were subjected to SDS-PAGE and western blot analysis.

Muscle tissues were homogenized in ice-cold lysis buffer (1 ml lysis buffer/100 mg tissue) without Triton X-100 using an Ultra-Turrax T10 Disperser (IKA) before Triton X-100 was added to the homogenates to reach a concentration of 1% (v/v). For analyses of TLR9 expression levels in tissues of TLR9–HA mice, mice were perfused with PBS before

being killed and subjected to tissue collection. Muscle homogenates were incubated at 4 °C for 1 h followed by centrifugation at 20,000g for 15 min. The supernatants were recovered as tissue lysates and precleared with protein A agarose (Sigma) for 1 h followed by immunoprecipitation of TLR9–HA, beclin 1 or UV-RAG. Anti-HA antibody (3724, Cell Signaling), anti-beclin 1 antibody (sc48341, Santa Cruz) or anti-UV-RAG antibody (11315, Cell Signaling) was added to the lysates for 3 h before protein A agarose was added for another 1.5 h. Immunoprecipitates were denatured with Laemmli buffer at 37 °C for 30 min before SDS-PAGE and western blot analysis.

Protein purifications

The maltose-binding-protein (MBP)-tagged TLR9 TIR domain (amino acids 868–1032) plasmid (a gift from J. Hurley) was used to re-clone the MBP-TLR9 TIR domain into the pCAG vector, removing the twin-Strep and Flag tags. One litre of HEK 293S cells (3.0×10^6 cells/ml) was transfected with the MBP-TIR plasmid using polyethylenimine (PEIpro) in the presence of 10 mM sodium butyrate (Sigma-Aldrich). After shaking for 48 h at 37 °C and 8% CO₂, cells were collected and lysed by adding 1% Triton X-100, followed by centrifugation at 50,000g for 30 min. The clear supernatant was collected, amylose resins (NEB) were added and incubated for 1 h at 4 °C. The resins were washed with 15 column volumes of the purification buffer (20 mM Tris pH 8.0, 150 mM NaCl and 1 mM DTT). The protein was eluted with purification buffer containing 10 mM maltose (Sigma-Aldrich) and subjected to size-exclusion chromatography. The eluate was pooled, concentrated, flash-frozen by liquid nitrogen and stored at -80 °C. The bacterial expression plasmid containing full-length human BECN1 (a gift from M. Ranaghan) was used to express and purify beclin 1 protein as previously described²⁵.

In vitro binding assays

Five hundred nanograms of MBP protein and MBP-TIR protein were incubated with 250 ng of beclin 1 protein in binding buffer (0.1% Triton, 1 mM DTT and 0.1% BSA in PBS) for 2 h at 4 °C before adding 50 µl of amylose resin (Bio-Rad) for another 2 h at 4 °C. After washing with binding buffer three times and with PBS twice, 100 µl of PBS containing 10 mM maltose was added to the resin for elution at room temperature for 15 min. The eluates were subjected to western blot analysis.

Western blot analysis

All primary antibodies used for western blots were purchased from commercial sources. Antibodies from Santa Cruz include: anti-beclin 1 (sc11427), anti-Myc HRP (sc40 HRP) and anti-β-actin HRP (sc47778 HRP). Antibodies from Cell Signaling Technology include: anti-UV-RAG (11315), anti-VPS34 (4263), anti-ATG14 (96752, to detect mouse ATG14), anti-p-AMPKα(T172) (2535), anti-AMPKα (2532), anti-p-raptor(S792) (2083), anti-raptor (2280), anti-TBC1D1 (66433) and anti-HA (3724, to detect TLR9–HA in tissue lysates of TLR9–HA mice). Other primary antibodies include: anti-p-ACC(S79) (07-303, Millipore), anti-ACC (04-322, Millipore), anti-p-TBC1D1(S237) (07-2268, Millipore), anti-ATG14 (M184-3, MBL International, to detect human ATG14), anti-HA high-affinity-HRP (12013819001, Roche, to detect overexpressed TLR9–HA in cells and TLR9–HA after immunoprecipitation from muscle lysates of the TLR9–HA mice), anti-Flag M2-HRP (A8592, Sigma), and anti-GLUT4 (GT41-A, Alpha Diagnostic International). To detect beclin 1 in TLR9–HA immunoprecipitates from muscle lysates by western blot analysis, 10% MINI-PROTEAN TGX precast gels (Bio-Rad) were used. For detection of all other proteins, 4–20% precast gels were used.

Exercise studies

Mouse treadmill exercise experiments were performed as previously described³ with minor modifications. Eight- to twelve-week-old mice were used for all experiments. In brief, mice were acclimated to the 10° uphill treadmill for two days. On day 1, mice ran for 5 min at a speed of 8 m/min followed by 2 min at a speed of 10 m/min. On day 2, mice ran for

5 min at a speed of 10 m/min followed by 2 min at a speed of 12 m/min. On day 3, mice were allowed to rest. On day 4, mice were subjected to a single bout of running starting at a speed of 10 m/min for 40 min. Afterwards, the speed was increased at a rate of 1 m/min every 10 min for a total of 30 min and then at a rate of 1 m/min every 5 min until reaching the designated time point (for tissue collection) or mouse exhaustion (for measurement of maximal running distance). Tissues were snap-frozen using liquid nitrogen at desired time points after exercise. For blood glucose measurements after exercise, food was removed from the mouse cages for 4 h before mice were subjected to treadmill exercise on day 4. Blood was obtained from the tail vein and blood glucose levels were measured using commercial glucose assay reagents (Sigma G6918, P7119 and F5803). For experiments involving the collection of muscle samples for immunoprecipitation, food was removed from the cages of the experimental mice at 18:00 on day 3, and then mice were refed ad libitum on day 4 for 3 h before treadmill running experiments were performed.

Bone marrow transplantation

Bone marrow transplantation experiments were performed as previously described²⁶. Donor bone-marrow cells were obtained from 8-week-old wild-type or *Tlr9*^{-/-} male mice and noncompetitively transplanted into irradiated 9- to 12-week-old wild-type or *Tlr9*^{-/-} male recipient mice. The recipient mice were irradiated using an XRAD 320 X-ray irradiator (Precision X-Ray) with two doses of 540 rad (1,080 rad in total) delivered at least 3 h apart. Two million donor bone-marrow cells were injected into the tail vein of each recipient mouse. Eight weeks after transplantation, high levels of donor-cell chimerism in the blood of recipient mice was confirmed using quantitative PCR (qPCR). Specifically, about 80 µl of blood was obtained from the tail vein of recipient mice and DNA was extracted using a QIAamp DNA mini kit (Qiagen). Then, 20 ng of DNA was used for qPCR using a SYBR green PCR kit (Qiagen) to determine the relative copy number of wild-type genome or *Tlr9*^{-/-} genome using the following primers: for wild-type genome, forward, 5'-GAAGGTTCTGGCTCAATGGTCATGTG-3'; reverse, 5'-GCAATGAAAGGACTGTCCACTTGTG-3'; for *Tlr9*^{-/-} genome, forward 5'-ATCGCCTTCTATGCCCTTCTGACGAG-3'; reverse, 5'-GCAATG GAAAGGACTGTCCACTTTGTG-3'. The relative copy numbers of *Tlr7* genome were used as an internal control for normalization. The following primers were used for the *Tlr7* genome: forward, 5'-AGGGTAT GCGCCAATCTAAAG-3'; reverse, 5'-ACCTTGTTGCTCCTGGAC-3'. Nine weeks after transplantation, recipient mice were used for exercise studies.

Ex vivo muscle studies

Ex vivo muscle incubation was performed as previously described^{27,28} with some modifications. Specifically, the feeding status of mice was synchronized by removing food overnight from their cages the day before experiments and replacing food for 4 h on the morning of the day when experiments were performed. Mice were anaesthetized by isoflurane inhalation and EDL muscles were dissected with the tendons at both ends ligated with 5-0 silk suture loops (F.S.T.) and suspended between two electrodes on a contraction apparatus at their resting length at 30 °C in modified Krebs–Ringer–Henseleit (KRH) buffer (120 mM NaCl, 4.74 mM KCl, 1.25 mM MgCl₂, 1.2 mM KH₂PO₄, 25 mM NaHCO₃, 1.25 mM CaCl₂, 5.5 mM glucose, 1 mM sodium pyruvate, 5 mM Hepes pH 7.4 and 0.1% bovine serum albumin) constantly gassed with 95% O₂/5% CO₂. To study the effects of TLR9 ligand on AMPK activation, muscles were pre-incubated for 45 min before treatment with 1 µM control ODN or ODN 2395 or 1 µM PF-739 (as positive control) for 1 h, followed by snap-freezing in liquid nitrogen. To study AMPK activation induced by muscle contractions, muscles were pre-incubated for 45 min before they were left resting or subjected to electrical stimulation (1-Hz, 30-V square wave pulses of 10-ms duration) for 20 min. Pulses were generated by a stimulus isolation amplifier (model 4AD, Getting

Article

Instruments) with the control of a waveform generator (model GH-CJDS66, Koolertron). Muscles were removed from the contraction apparatus and snap-frozen using liquid nitrogen. For measurement of glucose uptake during contraction, muscles were pre-incubated for 45 min before being subjected to electrical stimulation for 5 min. Muscles were then transferred into fresh KRH medium containing 0.25 µCi/ml [³H]2-deoxy-glucose (2DG) (PerkinElmer) and 0.1 µCi/ml [¹⁴C]mannitol (PerkinElmer) and subjected to electrical stimulation for another 15 min. For each electrically stimulated EDL muscle, the other EDL muscle from the same mouse was left resting for 15 min in the KRH medium containing [³H]2-deoxy-glucose and [¹⁴C]mannitol and used as a resting control. After treatments, muscles were collected, washed in ice-cold KRH medium, dabbed dry on filter paper and snap-frozen in liquid nitrogen. For 2DG uptake analysis, each muscle was homogenized in 600 µl ice-cold lysis buffer using an Ultra-Turrax as described in 'Lysate preparation and immunoprecipitation assays'. Then, 250 µl of lysate was mixed with 5 ml scintillation liquid (3a70B, RPI) to measure 2DG uptake by scintillation counting using [¹⁴C]mannitol for estimation of extracellular space.

Autophagy analyses

To assess autophagic flux in skeletal muscle in resting and exercise conditions, wild-type GFP-LC3 mice and *Tlr9*^{-/-};GFP-LC3 mice were acclimated to the treadmill as described in 'Exercise studies'. During the morning of day 4, mice were treated with either PBS or chloroquine (50 mg/kg) via intraperitoneal injection. For resting groups, after 3 h of PBS or chloroquine treatment, mice were anaesthetized by inhalational isoflurane and perfused with 30 ml 4% paraformaldehyde in PBS at a rate of 4.5 ml/min. Vastus lateralis muscles were collected and processed for frozen sectioning as previously described²². For exercise groups, after 90 min of PBS or chloroquine treatment, mice were subjected to treadmill running for 90 min before perfusion and muscle collection. Frozen muscle-section slides were air-dried at room temperature for 15 min before mounting and imaging by fluorescence microscopy using a Zeiss Axioplan2 microscope. The total number of GFP-LC3 puncta per 2,500 µm² was counted using ImageJ. More than 15 randomly chosen fields (by an observer blinded to experimental genotype) were used per mouse and an average value was determined.

Immunofluorescence analyses

For GLUT4 staining, wild-type and *Tlr9*^{-/-} mice were subjected to exercise for 95 min before perfusion and collection of muscles for frozen section preparation as described in 'Autophagy analyses'. Frozen muscle-section slides were heated at 50 °C for 15 min, rehydrated in PBS for 30 min, blocked with 1% BSA in PBS for 1 h and probed with anti-GLUT4 antibody (rabbit, GT41-A, Alpha Diagnostic International) and anti-laminin 2 antibody (rat, L0663, Sigma) overnight at 4 °C. Alexa-Fluor-594 anti-rabbit secondary antibody and Alexa-Fluor-488 anti-rat secondary antibody (Invitrogen) were then added for 1 h at room temperature before the slides were mounted and imaged using a Zeiss Axioplan2 microscope. Colocalization of GLUT4 and laminin was calculated using ImageJ. For muscle fibre-type staining and capillary density determination, tibialis anterior muscles were snap-frozen in liquid-nitrogen-cooled 2-methylbutane before being placed into OCT compound (Fisher Healthcare) and cryo-sectioned at a thickness of 10 µm. For muscle fibre-type staining, sections were blocked with 10% goat serum (Gibco) in PBS for 1 h at room temperature, and then probed with anti-myosin heavy chain type I (mouse, BA-D5, Developmental Studies Hybridoma Bank), anti-myosin heavy chain type IIa (mouse, SC-71, Developmental Studies Hybridoma Bank), anti-myosin heavy chain type IIb (mouse, BF-F3, Developmental Studies Hybridoma Bank) and anti-laminin (rabbit, L9393, Sigma) antibodies overnight at 4 °C. Alexa-Fluor-594 goat anti-mouse IgG1 (Invitrogen), Alexa-Fluor-647 goat anti-mouse IgG2b (Invitrogen), Alexa-Fluor-488 goat anti-rabbit

IgG (H+L) (Invitrogen) and Dylight 405 goat anti-mouse IgM (Jackson ImmunoResearch) secondary antibodies were then added for 1 h at room temperature before the slides were mounted and imaged using a Zeiss LSM780 inverted microscope. For capillary density determination, muscle sections were air dried at room temperature before being put into cold acetone (-20 °C) for 15 min. Slides were then washed 3 times with PBS and blocked with 1% BSA in PBS for 1 h before being probed with biotinylated lectin (5 µg/ml, B-1105, Vector Laboratories, to label capillary endothelial cells) and anti-laminin 2 antibody (rat, L0663, Sigma) overnight at 4 °C. Alexa-Fluor-488-conjugated streptavidin and Alexa-Fluor-594 anti-rat secondary antibody (Invitrogen) were then added for 1 h at room temperature before the slides were mounted and imaged using a Zeiss Axioplan2 microscope.

Muscle morphology and cytochrome c oxidase enzymatic activity

Fresh-frozen muscle sections were prepared as described in 'Immunofluorescence analyses' for muscle fibre-type staining. Haematoxylin and eosin (H&E) staining was performed following the protocol from the TREAT-NMD website (http://www.treat-nmd.eu/downloads/file/sops/cmd/MDC1A_M.1.2.004.pdf), and imaged using an Olympus IX83 microscope. Cytochrome c oxidase (COX) enzymatic activity was performed as previously described²⁹, and visualized using an Olympus IX83 microscope. COX stain intensity was calculated using ImageJ.

mtDNA and genomic DNA binding to TLR9-HA

Anti-HA high-affinity antibody (Roche) (1 µg/sample), protein G Dynabeads (Invitrogen) (50 µl/sample) and herring testes DNA (Sigma) (50 µg/sample) were added together and incubated at 4 °C overnight. The HA-antibody-bound beads were then washed once with lysis buffer before use in immunoprecipitation. Approximately 150 mg of gastrocnemius muscles from wild-type or TLR9-HA mice were homogenized as described in 'Lysate preparation and immunoprecipitation assays' using a lysis buffer containing 50 mM Hepes pH 7.4, 50 mM KCl, 50 mM NaF, 5 mM Na₄P₂O₇, 5 mM β-glycerophosphate, 1 mM EDTA, 1 mM EGTA, 1 mM Na₃VO₄, 1 mM DTT, 5% (v/v) glycerol supplemented with protease inhibitor cocktail (Roche) and 1% (v/v) NP40. Lysates were precleared with protein A agarose for 1 h and incubated with the prepared HA-antibody-bound beads at 4 °C overnight. The beads were then washed three times with lysis buffer. Approximately one-seventh of the beads were saved for western blot analysis to assess the amount of immunoprecipitated TLR9-HA; the remainder of the beads were resuspended in 80 µl nuclease-free water containing 200 µg/ml proteinase K (Roche) and incubated at 55 °C for 30 min followed by 95 °C for 15 min to inactivate proteinase K. After centrifugation at 12,000g for 5 min, the supernatants were collected and 5 µl of each sample was used for qPCR with each set of mtDNA primers using SYBR green PCR kit (Qiagen). The six sets of mouse mtDNA primers targeting different regions of the mitochondrial genome and two sets of genomic DNA primers have previously been described³⁰. mtDNA primer sets are: set 1 (targeting *mt-Nd1*), forward, 5'-CAAACACTTATT ACAACCAAGAAC-3'; reverse, 5'-TCATATTATGGCTATGGTCAGG-3'; set 2 (targeting *mt-Nd5*), forward, 5'-AGCATTCGGAAGCATTTG-3'; reverse, 5'-TTGTGAGGACTGGAATGCTG-3'; set 3 (targeting *mt-Nd5*), forward, 5'-CCACGCATTCTCAAAGCTA-3'; reverse, 5'-TCGGATGTCCTG TTGCTCTG-3'; set 4 (targeting *mt-Nd6*), forward, 5'-TGTTTGGGAG ATTGGTG-3'; reverse, 5'-CACAACTATATTGCCGCTACCC-3'; set 5 (targeting *mt-Rnr1*), forward, 5'-CCTCTTAGGGTTGGTAAATTG-3'; reverse, 5'-CGAAGATAATTAGTTGGGTTAATCG-3'; and set 6 (targeting *mt-Rnr2*), forward, 5'-AAACAGCTTTAACCATTTGAGGC-3'; reverse, 5'-TTGAGCTTGAACGCTTCTTA-3'. Genomic DNA primer sets are: set 1 (targeting *POLG*), forward, 5'-ATGAATGGGCCTACCTTGA-3'; reverse, 5'-TGGGTCCTGTTCTACAGC-3'; set 2 (targeting *POLG*), forward, 5'-TCCTCGAACAGTTGTGCTTC-3'; reverse, 5'-CCATCTA CTCAGGACGGAGTTC-3'.

mtDNA levels in plasma

Mouse blood was collected by cardiac puncture into EDTA-coated microtainers (BD). Plasma was obtained after two rounds of centrifugation (3,000g, 10 min at 4 °C). Then, 250 µl of plasma from each mouse was used to extract circulating DNA using QIAamp circulating nucleic acid kit (Qiagen). One-twentieth of the total yield from each plasma sample was used for qPCR to assess levels of mtDNA using six sets of mouse mtDNA primers as described in 'mtDNA and genomic DNA binding to TLR9–HA'.

qPCR

To assess mRNA levels of *Tlr9* in different tissues, qPCR analysis was performed on normalized mouse multiple-tissue cDNA panels (Takara) using SYBR green PCR kit (Qiagen). To compare mRNA levels of *Tlr9* in myoblast and myotubes, mouse primary myoblasts were isolated and differentiated into myotubes as previously described³¹. RNA was isolated from myoblasts and myotubes using RNeasy mini kit (Qiagen) and reverse-transcribed into cDNA using iScript cDNA synthesis kit (Bio-Rad) before use in qPCR analyses. The QuantiTect primer assay for mouse *Tlr9* (Qiagen) was used. The following primers were used for β-actin (*Actb*): forward, 5'-CTGGCTCCTAGCACCATGAAGAT-3'; reverse, 5'-GGTGGACAGTGAGGCCAGGAT-3'.

AMP, ADP and ATP measurements

Frozen EDL muscles were homogenized in 500 µl of ice-cold 0.1 M HClO₄/40% (v/v) CH₃OH using an Ultra-Turrax tissue disintegrator as described in 'Lysate preparation and immunoprecipitation assays'. After centrifugation (20,000g, 10 min at 4 °C), supernatants were neutralized with 1.1M (NH₄)₂HPO₄, dried and resuspended in high-performance liquid chromatography (HPLC)-grade water. Nucleotides were then separated and quantified by HPLC and UV detection as previously described³².

Measurement of muscle glycogen content

Mouse tibialis anterior muscles were homogenized with 600 µl of ddH₂O using an Ultra-Turrax tissue disintegrator as described in 'Lysate preparation and immunoprecipitation assays', before immediately placing them on a 95 °C heat block for 15 min to inactivate enzymes in the samples. After centrifugation (18,000g, 10 min at 4 °C), 5 µl of supernatant was used for the measurement of glycogen content using a Glycogen Assay kit (Abcam).

Mouse PF-739 treatment

The direct AMPK activator PF-739¹⁸ (AOBIOUS) was dissolved in DMSO at a concentration of 200 mg/ml. Before performing mouse experiments, a solution containing 10% 200 mg/ml PF-739 in DMSO/30% PEG 400/60% H₂O was prepared for subcutaneous injection into mice (50 µl per 10 g body weight). A solution containing 10% DMSO/30% PEG 400/60% H₂O was injected into control mice. Ninety minutes after injection, mice were anaesthetized by isoflurane inhalation and blood and tissues were collected for blood glucose measurement and western blot analyses.

Statistical analyses

Student *t*-tests and Mann–Whitney tests were performed using Prism software (GraphPad). One-way ANOVA and two-way ANOVA were

performed using R Project for Statistical Computing software. The Hommel method was used for post-hoc adjustment for multiple comparisons. The statistical methods used for each analysis are specified in the figure legends.

Reporting summary

Further information on research design is available in the Nature Research Reporting Summary linked to this paper.

Data availability

Full scans for all western blots are provided in Supplementary Fig. 1. Source Data for Figs. 1–3 and Extended Data Figs. 1–10 are provided with the paper. All other data are available from the corresponding author on reasonable request.

22. Mizushima, N., Yamamoto, A., Matsui, M., Yoshimori, T. & Ohsumi, Y. In vivo analysis of autophagy in response to nutrient starvation using transgenic mice expressing a fluorescent autophagosome marker. *Mol. Biol. Cell* **15**, 1101–1111 (2004).
23. Shoji-Kawata, S. et al. Identification of a candidate therapeutic autophagy-inducing peptide. *Nature* **494**, 201–206 (2013).
24. Lee, B. L. et al. UNC93B1 mediates differential trafficking of endosomal TLRs. *eLife* **2**, e00291 (2013).
25. Ranaghan, M. J. et al. The autophagy-related beclin-1 protein requires the coiled-coil and BAR domains to form a homodimer with submicromolar affinity. *Biochemistry* **56**, 6639–6651 (2017).
26. Agathocleous, M. et al. Ascorbate regulates haematopoietic stem cell function and leukaemogenesis. *Nature* **549**, 476–481 (2017).
27. Aslesen, R. & Jensen, J. Effects of epinephrine on glucose metabolism in contracting rat skeletal muscles. *Am. J. Physiol.* **275**, E448–E456 (1998).
28. Jensen, T. E. et al. PT-1 selectively activates AMPK-γ1 complexes in mouse skeletal muscle, but activates all three γ subunit complexes in cultured human cells by inhibiting the respiratory chain. *Biochem. J.* **467**, 461–472 (2015).
29. Chen, H. et al. Mitochondrial fusion is required for mtDNA stability in skeletal muscle and tolerance of mtDNA mutations. *Cell* **141**, 280–289 (2010).
30. White, M. J. et al. Apoptotic caspases suppress mtDNA-induced STING-mediated type I IFN production. *Cell* **159**, 1549–1562 (2014).
31. Millay, D. P. et al. Myomaker is a membrane activator of myoblast fusion and muscle formation. *Nature* **499**, 301–305 (2013).
32. Plaideau, C. et al. Effects of pharmacological AMP deaminase inhibition and *Ampd1* deletion on nucleotide levels and AMPK activation in contracting skeletal muscle. *Chem. Biol.* **21**, 1497–1510 (2014).

Acknowledgements We thank R. Bassel-Duby, C. He, R. Medzhitov and P. Scherer for helpful discussions; C. Chang, J. Doenich, G. Barton, J. Jensen, J. Hurley, N. Mizushima, M. Ranaghan and F. Yarovinsky for providing critical reagents; L. Nguyen for technical assistance; and L. Bennett and H. Smith for assistance with manuscript preparation. This work was supported by NIH grants RO1 CA109618 (B.L.), U19 AI109725 (B.L.) and U19 AI142784 (B.L.); Cancer Prevention Research Institute of Texas grant RP120718 (B.L.); and a Fondation Leducq grant 15CBD04 (B.L.). M.J. was supported by a chargé de recherche post-doctoral grant from the Belgian F.N.R.S.

Author contributions Y.L., S.S.-K., M.H.R., S.J.M., P.M. and B.L. designed the study. Y.L., P.T.N., X.W., Y.Z., C.E.M., Z.Z., B.B., M.J., D.V., T.W., H.M. and S.S.-K. performed the experiments. Y.L., G.X. and B.L. analysed the data. Y.L. and B.L. wrote the manuscript.

Competing interests B.L. is a Scientific Co-Founder of Casma Therapeutics, Inc.

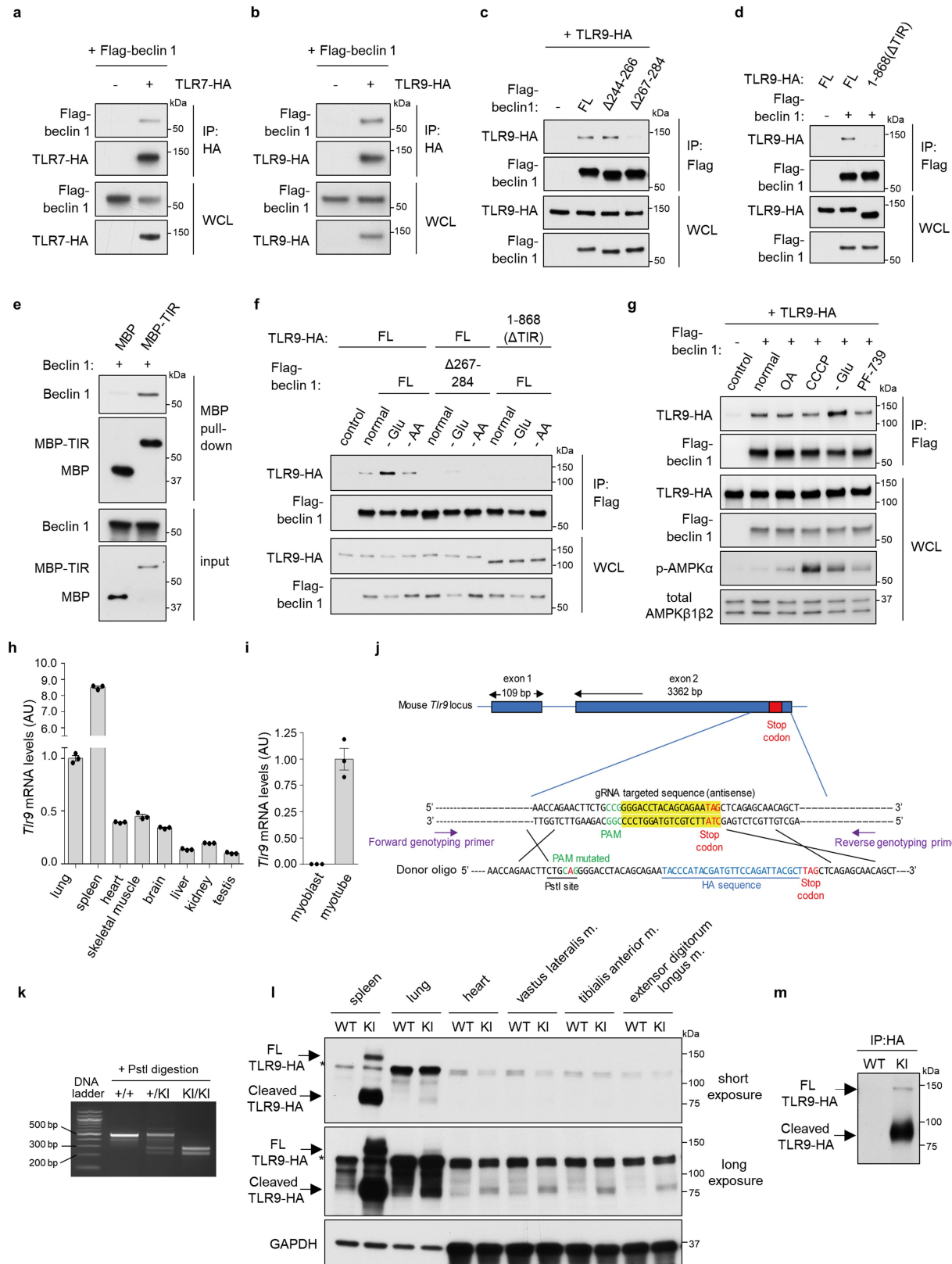
Additional information

Supplementary information is available for this paper at <https://doi.org/10.1038/s41586-020-1992-7>.

Correspondence and requests for materials should be addressed to Y.L. or B.L.

Reprints and permissions information is available at <http://www.nature.com/reprints>.

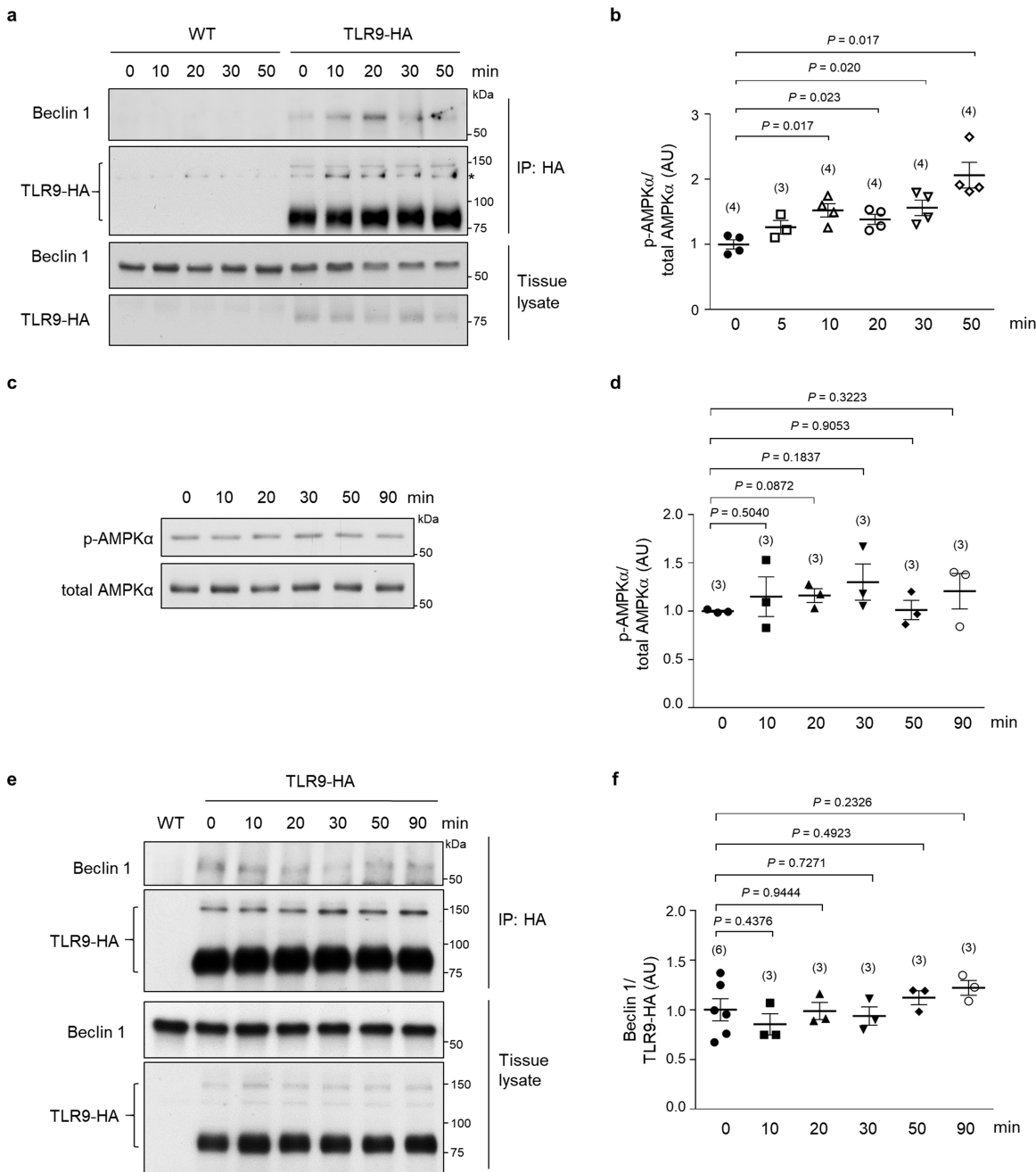
Article



Extended Data Fig. 1 | See next page for caption.

Extended Data Fig. 1 | TLR7 and TLR9 interaction with beclin 1 and generation of TLR9–HA mice. **a, b**, Co-immunoprecipitation of Flag–beclin 1 with TLR7–HA (**a**) or TLR9–HA (**b**) in transfected HeLa cells. **c**, Co-immunoprecipitation of TLR9–HA with Flag–full-length (FL) beclin 1 or deletion-mutant proteins in transfected U2OS cells. Flag–beclin 1(Δ244–266) is a control deletion mutant. **d**, Co-immunoprecipitation of TLR9–HA full-length protein or truncation mutant that lacks the TIR domain (1–868(ΔTIR)) with Flag–beclin 1 in transfected U2OS cells. **e**, MBP pull-down of recombinant beclin 1 with a protein comprising MBP fused to the TIR domain of TLR9 (MBP-TIR). **f**, Co-immunoprecipitation of indicated TLR9–HA constructs with indicated Flag–beclin 1 constructs in transfected U2OS cells cultured in normal medium, or subjected to 1 h glucose (−glu) or amino acid (−AA) starvation. **g**, Co-immunoprecipitation of TLR9–HA with Flag–beclin 1 in transfected U2OS cells cultured in normal medium, subjected to glucose starvation (for 1 h) or treatment for 1 h with the mitochondrial damaging agents oligomycin (2.5 μM) + antimycin A (250 nM) (OA) or CCCP (5 μM), or the direct AMPK activator PF-739 (5 μM). In **a–g**, results are representative of three independent

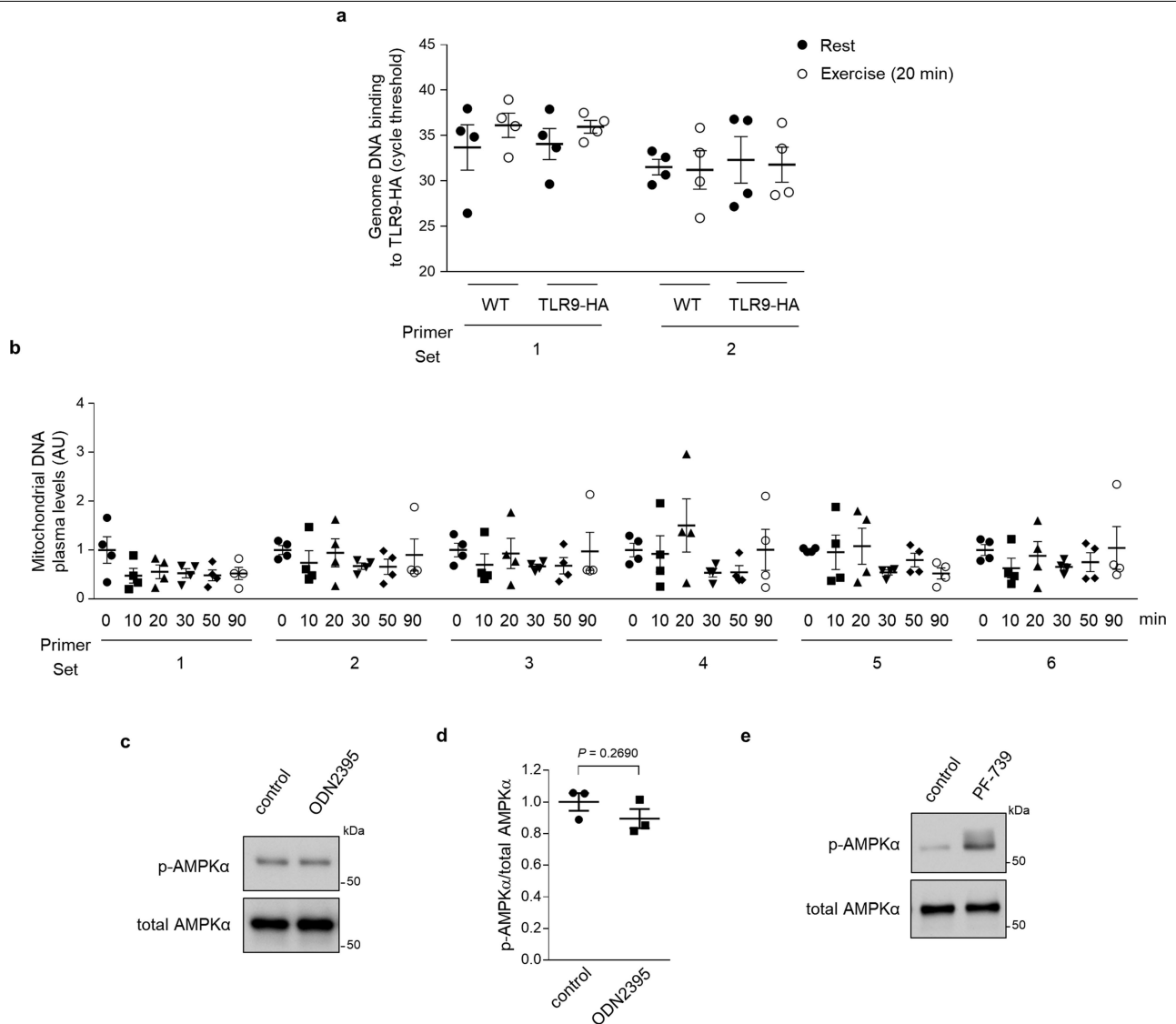
experiments. **h**, *Tlr9* mRNA levels in different tissues. The value in lung tissue is considered to be 1. **i**, *Tlr9* mRNA levels in myoblasts and myotubes (before and after myocyte differentiation, respectively) normalized to levels of β-actin. The value in myotubes is considered to be 1. In **h, i**, data are mean ± s.e.m. of triplicate samples. **j**, Schematic of the *Tlr9* locus and CRISPR-based gene knock-in strategy (Methods). **k**, Representative genotyping of wild-type (+/+), heterozygous knock-in (+/KI) and homozygous knock-in (KI/KI) mice. **l**, Western blots of TLR9–HA expression in indicated tissues from mice (loading amount for spleen and lung, 20 μg; for heart and muscle, 50 μg). Full-length (approximately 130 kDa) and cleaved (approximately 80 kDa) TLR9 detected in spleen. In the skeletal muscle and heart tissues, only the predominant cleaved form of TLR9 was detected, owing to lower levels of TLR9 expression. Asterisk denotes a nonspecific band. **m**, Western blot indicating that full-length and cleaved TLR9 are detected in muscle lysates after enriching by immunoprecipitation with anti-HA antibody. For **k–m**, similar results were observed in three independent experiments. For uncropped gels, see Supplementary Fig. 1.



Extended Data Fig. 2 | TLR9–beclin 1 interaction and AMPK phosphorylation increases in skeletal muscle, but not in spleen, during exercise.

a, Representative western blots of endogenous beclin 1 co-immunoprecipitated with endogenous TLR9- α H in vastus lateralis muscles from TLR9- α H mice and wild-type mice (negative control) at indicated durations of exercise. Asterisk denotes a nonspecific band also observed in wild-type mice. Similar results were observed in three independent experiments. **b**, Quantification of p-AMPK α (T172)/total AMPK α (representative blots are shown in Fig. 1b) in vastus lateralis muscles from TLR9- α H mice at indicated durations of exercise. Results are combined data from three independent experiments with similar results in each experiment.

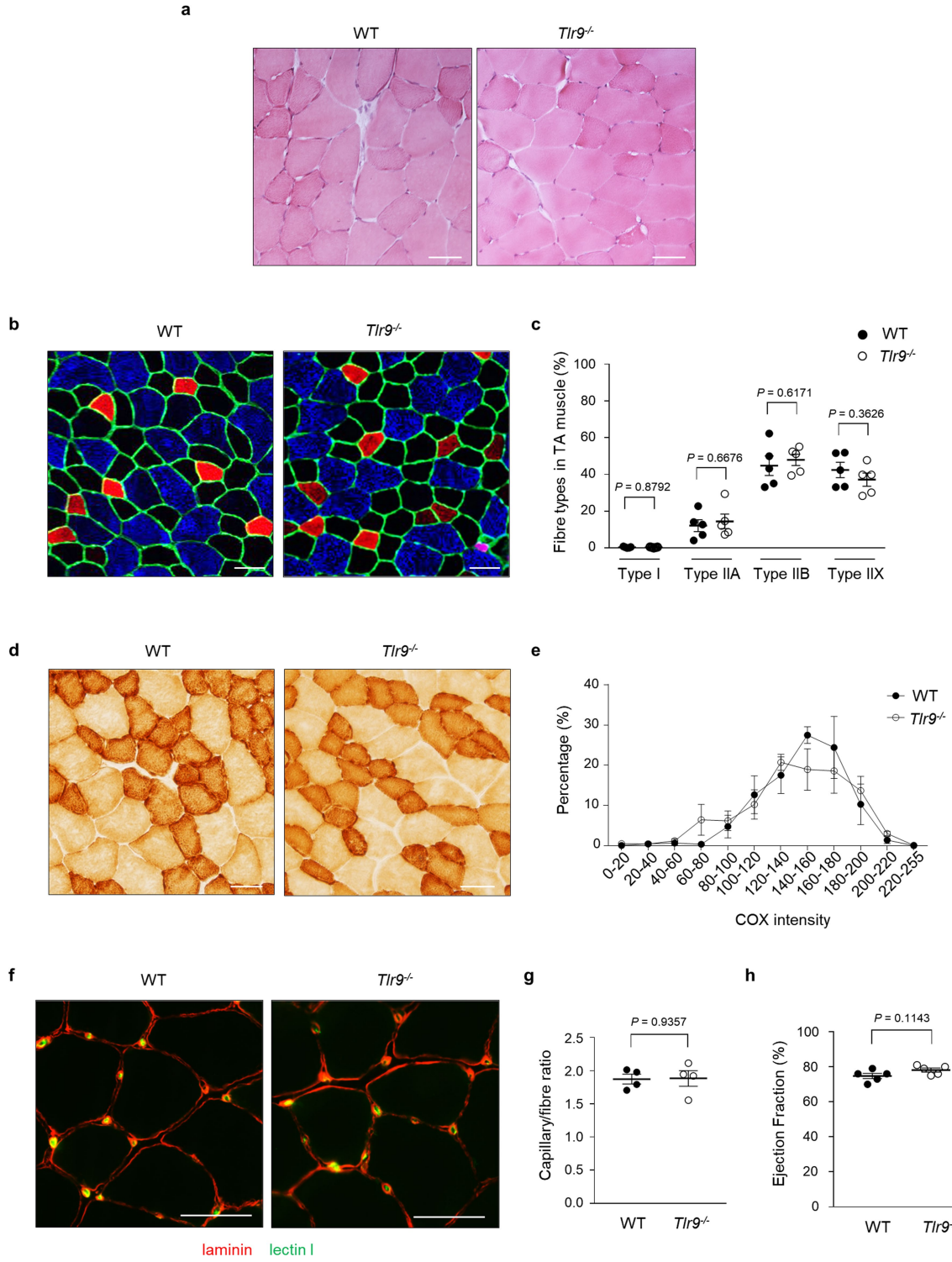
c, d, Representative blots (c) and quantification (d) of p-AMPK α (T172)/total AMPK α in the spleen of TLR9-HA mice at indicated durations of exercise. Results are combined data from two independent experiments with similar results in each experiment. **e, f**, Representative western blots (e) and quantification (f) of beclin 1 co-immunoprecipitated with TLR9-HA in spleens from TLR9-HA mice at indicated durations of exercise. Results are combined data from two independent experiments with similar results in each experiment. In **b, d, f**, data points are individual mice (sample size is indicated in parentheses). Data are mean \pm s.e.m. Values at 0 min are considered to be 1. In **b, d, f**, unpaired two-tailed *t*-test with Hommel method. For uncropped gels, see Supplementary Fig. 1.



Extended Data Fig. 3 | Levels of genomic DNA associated with TLR9 in skeletal muscle, levels of plasma mtDNA, and effects of treatment with exogenous TLR9 ligand on AMPK phosphorylation in skeletal muscle.

a, qPCR quantification of genomic DNA bound to TLR9. Cycle threshold (C_t) values for genomic DNA that co-immunoprecipitates with TLR9-HA from gastrocnemius muscles of wild-type or TLR9-HA mice at rest or after 20 min exercise are shown. Two sets of genomic DNA primers (Methods) were used. **b**, Quantification of mtDNA in plasma at serial time points after exercise in wild-type mice. The amount of mtDNA was quantified by qPCR using six sets of mtDNA primers (Methods). For each primer set, the value at the 0-min time point is considered to be 1. In **a**, **b**, data are mean \pm s.e.m.; data points are individual mice ($n=4$). **c**, **d**, Representative blots (**c**) and quantification (**d**) of

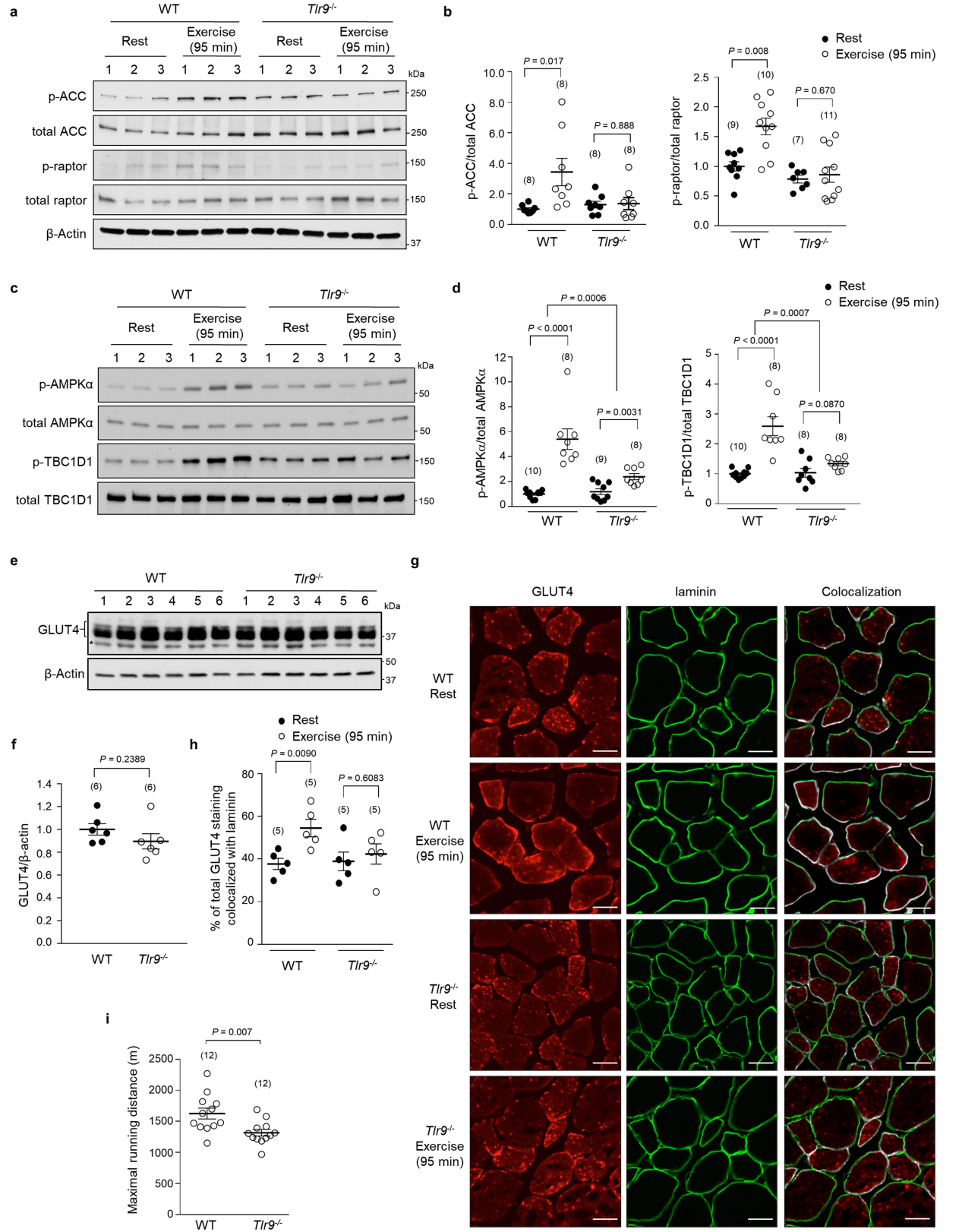
p-AMPK(T172)/total AMPK in EDL muscles from wild-type mice incubated ex vivo with 1 μ M control ODN or ODN2395 (a TLR9 ligand) for 1 h. Data are mean \pm s.e.m. Data points are individual muscles ($n=3$). Unpaired two-tailed t -test. Western blots are from one representative experiment, and quantification data are combined from three independent experiments. Similar results were observed in each experiment. **e**, Western blot of AMPK phosphorylation at Thr172 in EDL muscles from wild-type mice incubated with or without 1 μ M PF-739 (a direct AMPK activator) for 1 h. PF-739 is a positive control for experiments in **c** and **d** with respect to AMPK activation in EDL muscles ex vivo. Similar results were observed in three independent experiments. For uncropped gels, see Supplementary Fig. 1.



Extended Data Fig. 4 | Wild-type and Tlr9^{-/-} mice display similar muscle characteristics and cardiac function. **a, b,** Representative H&E staining (**a**) and fibre-type staining (**b**) of tibialis anterior muscles. In **b**, green denotes a plasma membrane marker (laminin); pink, type-I fibres (MHC I-positive); red, type-IIA fibres (MHC II A-positive); blue, type-IIB fibres (MHC II B-positive); and black, type-IIX fibres. **c**, Relative quantification of fibre-type composition in tibialis anterior muscles shown in **b**. Data are mean \pm s.e.m. At least 1,400 muscle fibres were analysed per mouse. **d, e,** Representative images (**d**) and quantification (**e**) of staining for COX enzymatic activity (a measure of mitochondrial respiratory capacity) in tibialis anterior muscles. Data are

mean \pm s.e.m. At least 480 muscle fibres were analysed per mouse.

f, g, Representative images (**f**) and quantification (**g**) of capillary density in tibialis anterior muscles. Data are mean \pm s.e.m. At least 240 muscle fibres were analysed per mouse. **h,** Cardiac function determined by echocardiographic measurement of ejection fraction. For **a, b, d, f**, images are representative from one of two independent experiments. Similar results were observed in each experiment. Data are mean \pm s.e.m. For **c, g, h**, data points are individual mice ($n=5$ mice per group for **c, h**; $n=4$ mice per group for **g**). For **e**, data points are the average values of five mice. Unpaired two-tailed *t*-test. Scale bars, 50 μ m.

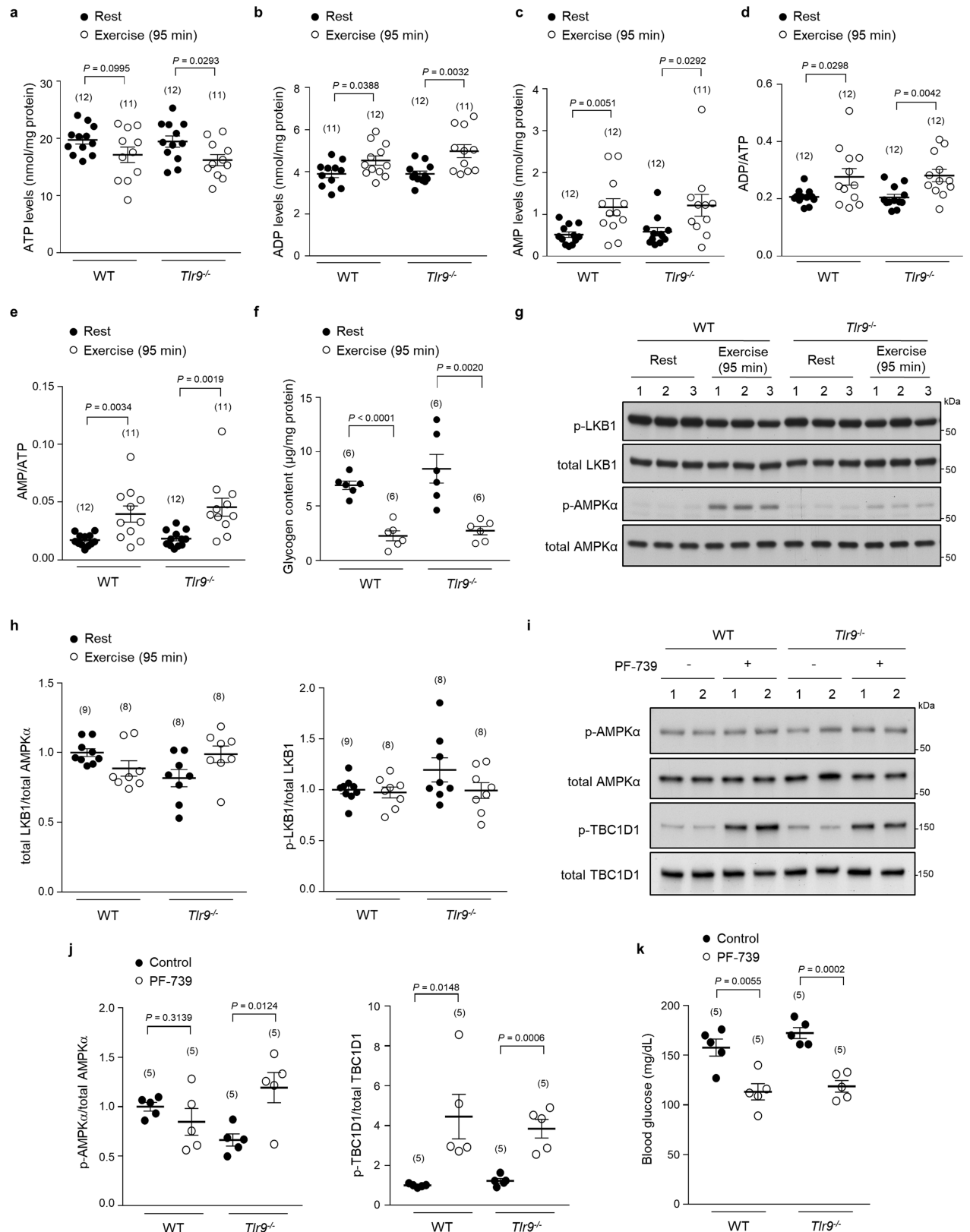


Extended Data Fig. 5 | See next page for caption.

Article

Extended Data Fig. 5 | Measurement of exercise-induced activation of AMPK in muscles, exercise-induced localization of GLUT4 to the plasma membrane in muscles, and maximal running distance in wild-type and *Tlr9*^{-/-} mice. **a, b,** Representative western blots (**a**) and quantification (**b**) of the phosphorylation of AMPK substrates (ACC at Ser79 and raptor at Ser792) in vastus lateralis muscles. The samples in **a, b** are the same as those used in Fig. 2a, b. **c, d,** Representative western blots (**c**) and quantification (**d**) of p-AMPK and p-TBC1D1 in EDL muscles. **e, f,** Western blots (**e**) and quantification (**f**) of GLUT4 levels in EDL muscles. Asterisk denotes a nonspecific band. **g,** Representative images of GLUT4 (red) and laminin (green) immunofluorescent staining (used for quantification in **h** and Fig. 2d) in EDL muscles. White denotes colocalization between GLUT4 and laminin as determined using ImageJ software. Scale bars, 20 μm. **h,** Percentage of total

GLUT4 staining colocalized with laminin calculated using ImageJ software. At least 100 muscle fibres were analysed per mouse. **i,** Maximal running distance. Data are combined from three independent experiments. Similar results were observed in each experiment. For **b, d, f, h, i**, data are mean ± s.e.m.; data points are individual mice (sample size indicated in parentheses). In **a–d, g, h**, western blots and images are from one representative experiment, and quantifications are combined data from three independent experiments. Similar results were observed in each experiment. In **b, d, h**, a two-tailed *t*-test was used to compare different conditions for each genotype and two-way ANOVA was used to compare magnitude of changes between different conditions in mice of different genotypes. In **f, i**, an unpaired two-tailed *t*-test was used. For uncropped gels, see Supplementary Fig. 1.



Extended Data Fig. 6 | See next page for caption.

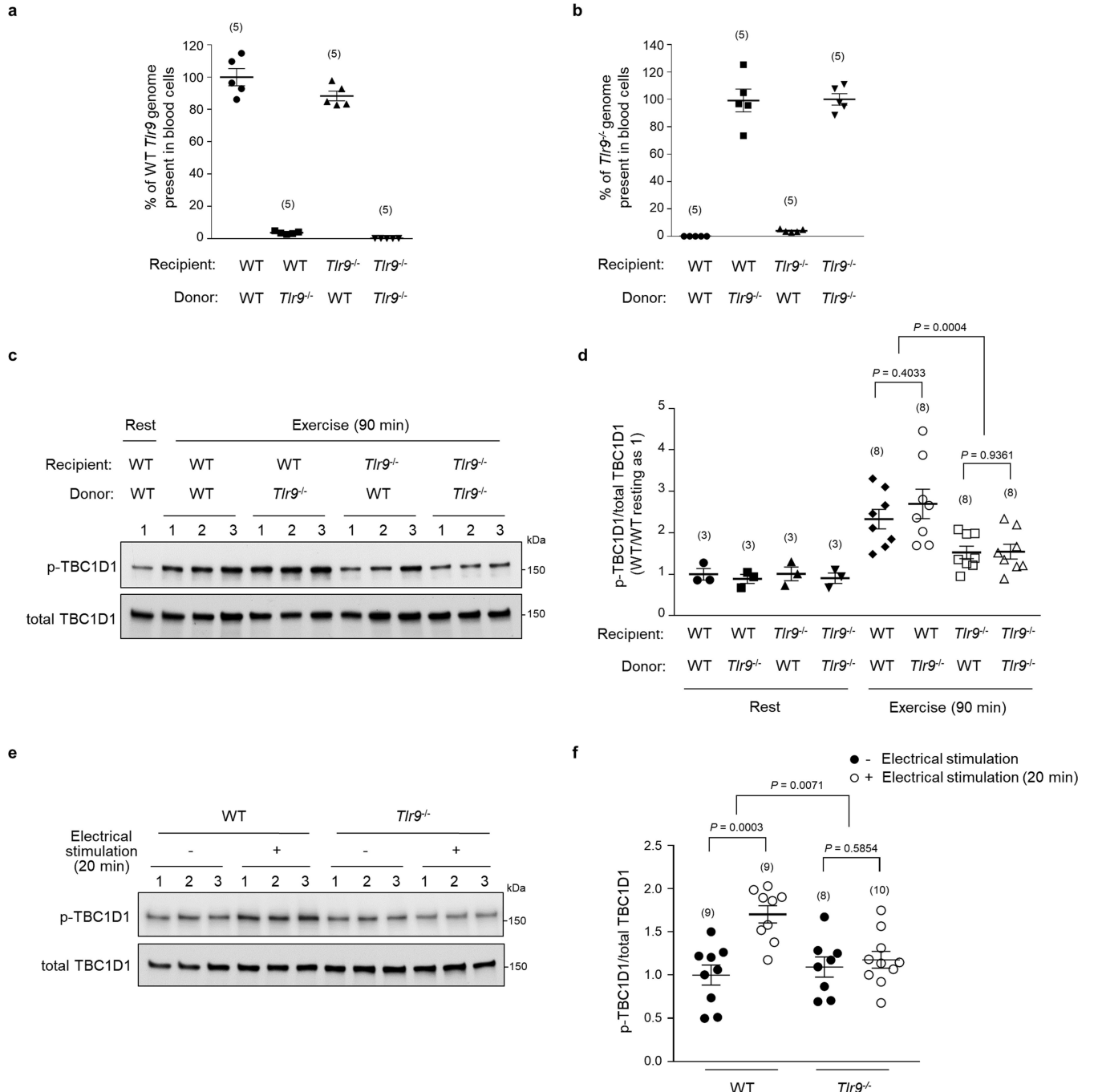
Article

Extended Data Fig. 6 | Similar levels of adenine nucleotides, glycogen, total LKB1 and LKB1 phosphorylation at Ser428, and a similar response to an AMPK allosteric activator in wild-type and *Tlr9*^{-/-} muscles.

a–e, Measurements of ATP (**a**), ADP (**b**), AMP (**c**), ADP/ATP ratio (**d**) and AMP/ATP ratio (**e**) in EDL muscles. **f**, Glycogen content in tibialis anterior muscles.

g, h, Representative western blots (**g**) and quantification (**h**) of p-LKB1(S428) and total LKB1 in vastus lateralis muscles. Representative blots are from one experiment, and quantification data are combined from three independent experiments. Similar results were observed in each experiment.

i, j, Representative western blots (**i**) and quantification (**j**) of AMPK activation markers (p-AMPK and p-TBC1D1) in tibialis anterior muscles of mice, 90 min after subcutaneous administration of PF-739 (100 mg per 5 ml, per kg body weight). **k**, Blood glucose levels 90 min after treatment with PF-739. In **i–k**, western blots are from one representative experiment, and quantification results are combined data from two independent experiments. Similar results were observed in each experiment. Data points are individual mice (sample size indicated in parentheses). Data are mean ± s.e.m. Unpaired two-tailed *t*-test. For uncropped gels, see Supplementary Fig. 1.

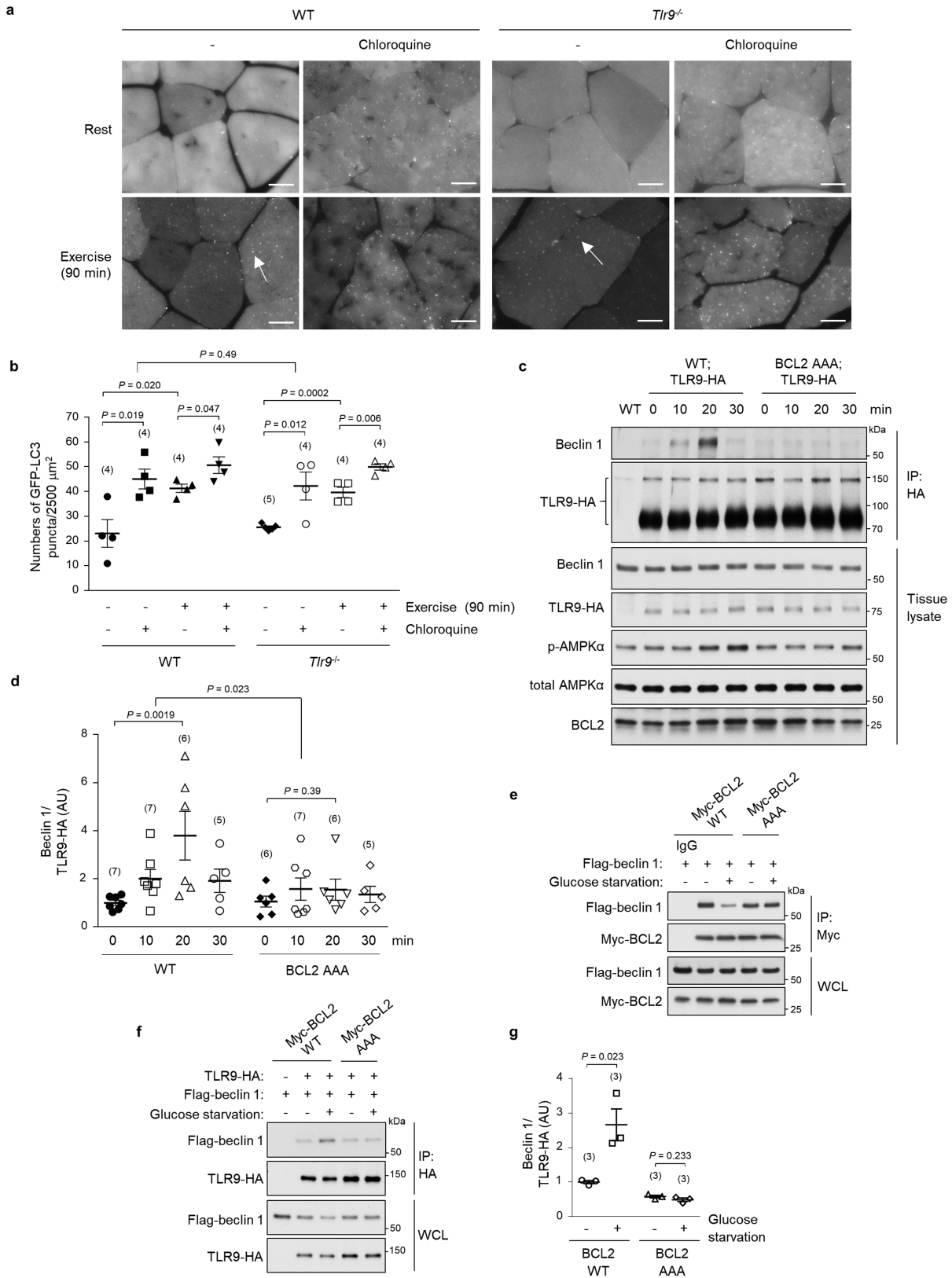


Extended Data Fig. 7 | Haematopoietic cells are not responsible for the defect in exercise-induced activation of AMPK in *Tlr9^{-/-}* muscles, and TLR9 is required for ex vivo electrical-stimulation-induced activation of AMPK.

a, b, Percentage of wild-type *Tlr9* genome (**a**) or *Tlr9^{-/-}* genome (**b**) in blood cells from mice with indicated donor or recipient genotypes at eight weeks after bone marrow transplantation, as determined by qPCR. The copy number of *Tlr7* genome is used as an internal control. Data are mean \pm s.e.m. for five randomly selected mice per group. Data points are individual mice. The mean of wild-type–wild-type (**a**) or *Tlr9^{-/-}*–*Tlr9^{-/-}* (**b**) donor–recipient combinations was considered to be 100%. **c, d**, Representative western blots (**c**) and quantification (**d**) of phosphorylation of TBC1D1 at Ser237 in vastus lateralis muscles of indicated recipient mice transplanted with indicated bone marrow cells, at rest and after 90 min exercise. **e, f**, Representative western blots (**e**) and

quantification (**f**) of phosphorylation of TBC1D1 at Ser237 in EDL muscles of wild-type and *Tlr9^{-/-}* mice with or without 20 min of electrical stimulation. In **c–f**, western blots are from one representative experiment, and quantification results are combined data from three independent experiments. Similar results were observed for each experiment. Data points are individual mice (**d**) or muscles (**f**) (sample size indicated in parentheses). Data are mean \pm s.e.m. In **d**, an unpaired two-tailed *t*-test was used to compare differences between donor genotypes, and a two-way ANOVA was used to compare differences between recipient genotypes. In **f**, an unpaired two-tailed *t*-test was used to compare conditions with and without electrical stimulation, for each genotype. A two-way ANOVA was used to compare the magnitude of changes between conditions with and without electrical stimulation in muscles of different genotypes. For uncropped gels, see Supplementary Fig. 9.

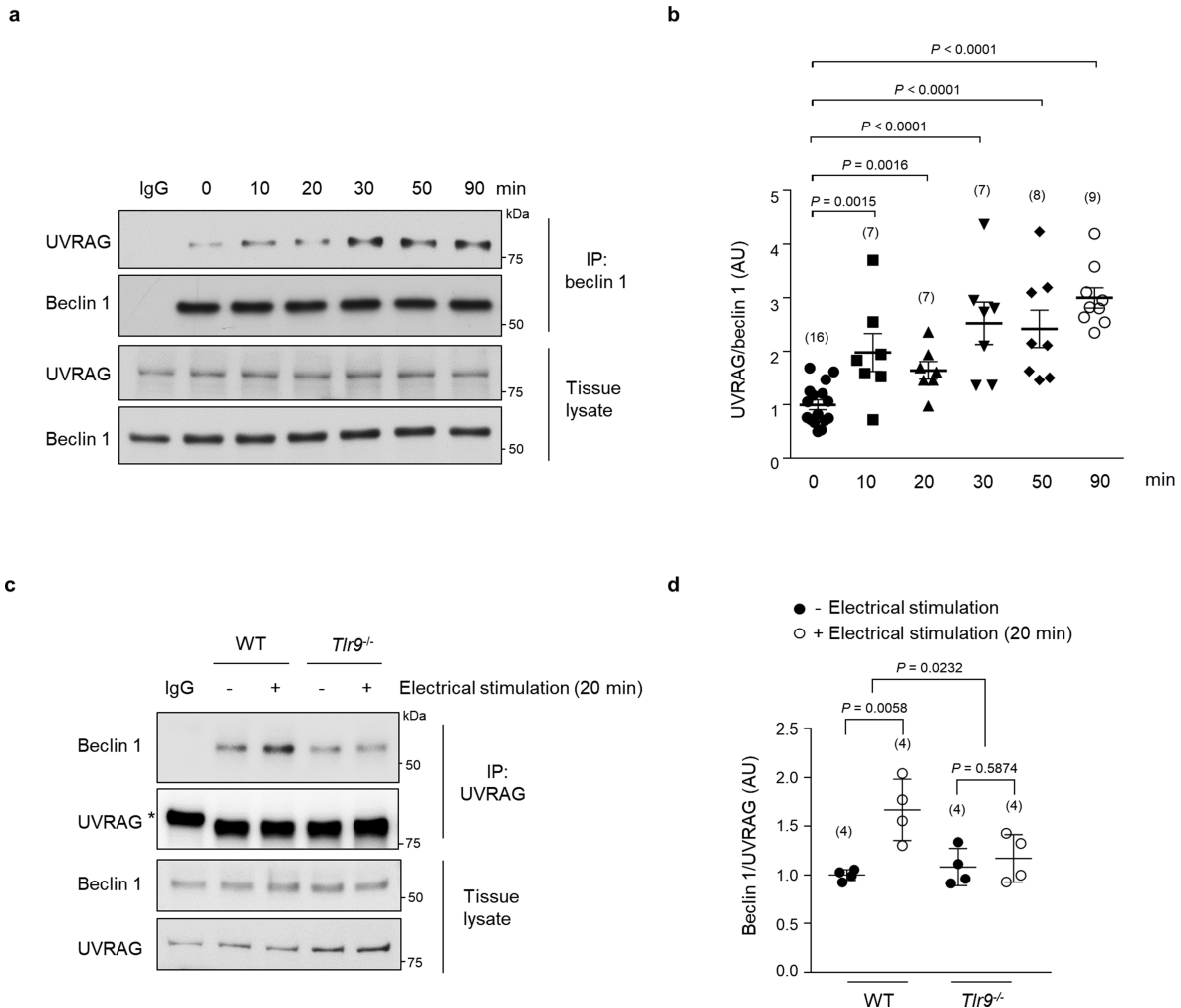
Article



Extended Data Fig. 8 | See next page for caption.

Extended Data Fig. 8 | *Tlr9^{-/-}* mice have normal exercise-induced autophagy, and BCL2 binding to beclin 1 inhibits the beclin 1-TLR9 interaction induced by exercise or glucose starvation. **a, b**, Representative images (**a**) and quantification (**b**) of GFP-LC3 puncta in vastus lateralis muscles of wild-type GFP-LC3 and *Tlr9^{-/-}*;GFP-LC3 mice at rest or after exercise, with and without chloroquine pretreatment. Scale bars, 20 μ m. Arrows mark representative puncta, counted in **b**. More than 15 randomly chosen fields were used per mouse and an average value was determined for each mouse. Images are from one representative experiment, and quantitative data are the combined results of two independent experiments. Similar results were observed in each experiment. Data points are individual mice (sample size in parentheses). **c, d**, Representative western blots (**c**) and quantification (**d**) of beclin 1 co-immunoprecipitated with TLR9-HA at serial time points after exercise in vastus lateralis muscles of TLR9-HA mice crossed to either BCL2 AAA mice or wild-type littermates. Western blots are from one representative experiment, and quantification data are the combined results from three independent experiments. Similar results were observed in each experiment. Data points

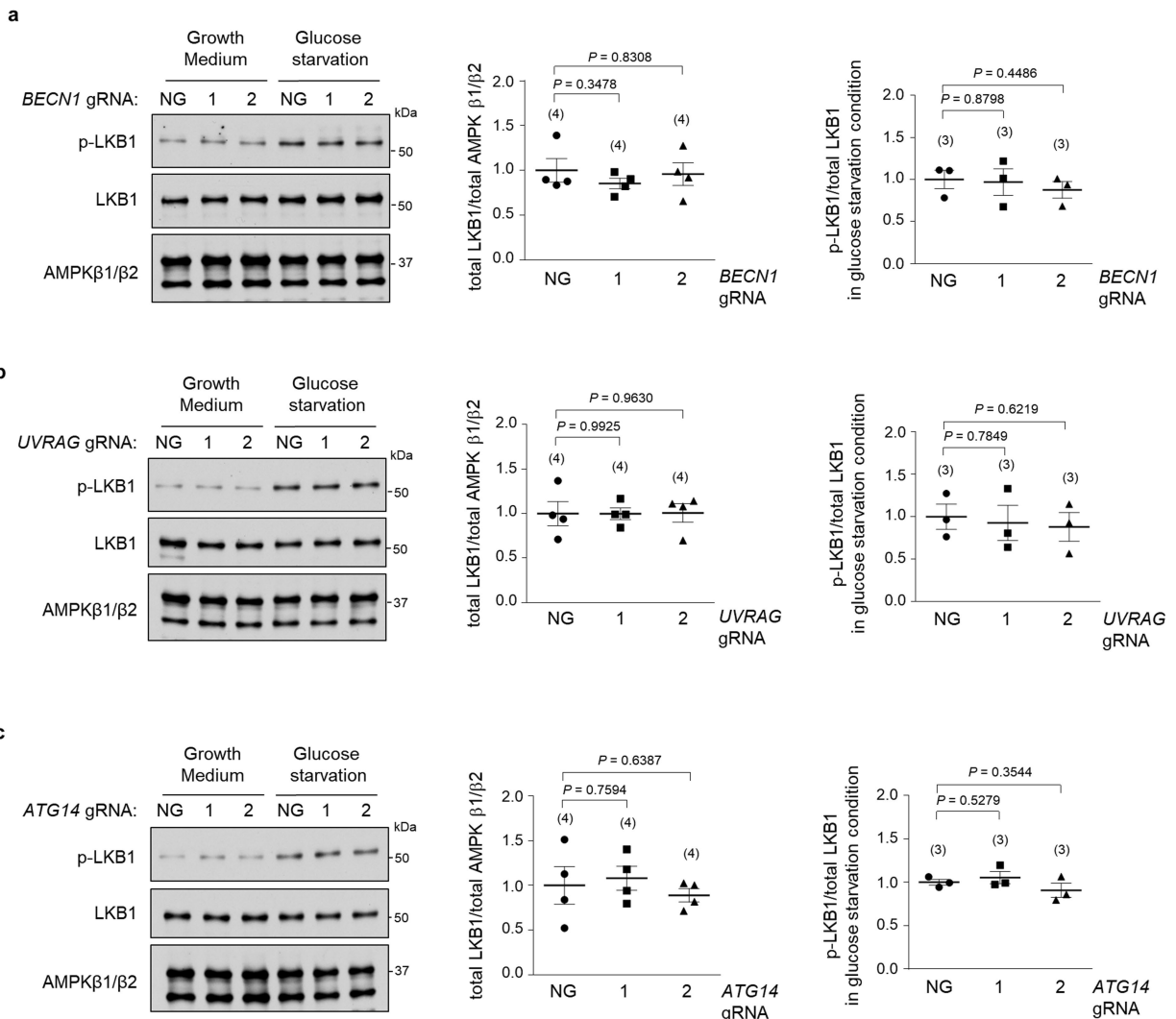
are individual mice (sample size in parentheses). **e**, Co-immunoprecipitation of transiently expressed Flag-beclin 1 with Myc-BCL2 in HeLa cells stably expressing wild-type Myc-BCL2 or BCL2 AAA¹⁹ grown in normal medium or subjected to 2-h glucose starvation. Similar results were observed in three independent experiments. **f, g**, Representative western blots (**f**) and quantification (**g**) of Flag-beclin 1 co-immunoprecipitated with TLR9-HA in HeLa cells stably expressing wild-type Myc-BCL2 or BCL2 AAA grown in normal medium or subjected to 2-h glucose starvation. Data are mean \pm s.e.m. from three experiments; sample size is indicated in parentheses. In **b**, an unpaired two-tailed *t*-test was used to compare different conditions for each genotype. A two-way ANOVA was used to compare the magnitude of changes between different conditions in mice of different genotypes. In **d**, a one-way ANOVA was used to compare 0-min and 20-min exercise conditions for each genotype. A two-way ANOVA was used to compare the magnitude of changes between 0-min and 20-min exercise conditions in mice of different genotypes. In **g**, an unpaired two-tailed *t*-test was used. For uncropped gels, see Supplementary Fig. 1.



Extended Data Fig. 9 | The beclin 1 and UVRAG interaction increases during exercise and during muscle contractions induced by electrical stimulation.

a, b. Representative blots (**a**) and quantification (**b**) of UVRAG co-immunoprecipitated with beclin 1 in tibialis anterior muscles of wild-type mice at indicated durations of exercise. Western blots are from one representative experiment, and quantification data are the combined results from five independent experiments. Similar results were observed in each experiment. **c, d.** Representative blots (**c**) and quantification (**d**) of beclin 1 co-immunoprecipitated with UVRAG in EDL muscles of wild-type and *Tlr9*^{-/-} mice with or without 20 min of electrical stimulation. Western blots are from one

representative experiment, and quantification data are the combined results from two independent experiments. Similar results were observed in each experiment. In **b, d**, data points are individual mice (**b**) or muscle (**d**) (sample size indicated in parentheses). Data are mean \pm s.e.m. In **b**, an unpaired two-tailed *t*-test was used. In **d**, a two-tailed *t*-test was used to compare conditions with and without electrical stimulation for each genotype. A two-way ANOVA was used to compare the magnitude of changes in conditions with and without electrical stimulation in muscles of different genotypes. Asterisk denotes a nonspecific band observed in IgG control condition. For uncropped gels, see Supplementary Fig. 1.



Extended Data Fig. 10 | Beclin 1, UVRAG or ATG14 knockout does not affect levels of LKB1 protein or the phosphorylation of LKB1 at Ser428 induced by glucose starvation. a–c, Effects of beclin1 (a), UVRAG (b) or ATG14 (c) knockout in U2OS cells on levels of LKB1 protein and phosphorylation of LKB1 at Ser428, 1 h after glucose starvation. Left, representative western blots of p-LKB1, total LKB1 and total AMPK β in cells with indicated gene knockout (two

independent gRNAs per target gene). Right, quantification of total LKB1/total AMPK β (from four independent experiments) and p-LKB1/total LKB1 (from three independent experiments). Similar results were observed in each experiment. Data are mean \pm s.e.m. Sample size is indicated in parentheses. Unpaired two-tailed t -test. NG, no gRNA. For uncropped gels, see Supplementary Fig. 1.

Reporting Summary

Nature Research wishes to improve the reproducibility of the work that we publish. This form provides structure for consistency and transparency in reporting. For further information on Nature Research policies, see [Authors & Referees](#) and the [Editorial Policy Checklist](#).

Statistical parameters

When statistical analyses are reported, confirm that the following items are present in the relevant location (e.g. figure legend, table legend, main text, or Methods section).

n/a Confirmed

- The exact sample size (n) for each experimental group/condition, given as a discrete number and unit of measurement
- An indication of whether measurements were taken from distinct samples or whether the same sample was measured repeatedly
- The statistical test(s) used AND whether they are one- or two-sided
Only common tests should be described solely by name; describe more complex techniques in the Methods section.
- A description of all covariates tested
- A description of any assumptions or corrections, such as tests of normality and adjustment for multiple comparisons
- A full description of the statistics including central tendency (e.g. means) or other basic estimates (e.g. regression coefficient) AND variation (e.g. standard deviation) or associated estimates of uncertainty (e.g. confidence intervals)
- For null hypothesis testing, the test statistic (e.g. F , t , r) with confidence intervals, effect sizes, degrees of freedom and P value noted
Give P values as exact values whenever suitable.
- For Bayesian analysis, information on the choice of priors and Markov chain Monte Carlo settings
- For hierarchical and complex designs, identification of the appropriate level for tests and full reporting of outcomes
- Estimates of effect sizes (e.g. Cohen's d , Pearson's r), indicating how they were calculated
- Clearly defined error bars
State explicitly what error bars represent (e.g. SD, SE, CI)

Our web collection on [statistics for biologists](#) may be useful.

Software and code

Policy information about [availability of computer code](#)

Data collection

No software was used.

Data analysis

The Image J software (Fiji version) was used to quantify the intensities of the bands in western blots, to count the numbers of GFP-LC3 puncta per 2,500 square μm of area and to quantify the colocalization between GLUT4 and Laminin. GraphPad Prism 7 was used to represent data in graphs and perform the Student's t-test and Mann-Whitney test. R Project for Statistical Computing software (version 3.6.1) was used to perform one-way ANOVA and two-way ANOVA statistical analysis of the data.

For manuscripts utilizing custom algorithms or software that are central to the research but not yet described in published literature, software must be made available to editors/reviewers upon request. We strongly encourage code deposition in a community repository (e.g. GitHub). See the Nature Research [guidelines for submitting code & software](#) for further information.

Data

Policy information about [availability of data](#)

All manuscripts must include a [data availability statement](#). This statement should provide the following information, where applicable:

- Accession codes, unique identifiers, or web links for publicly available datasets
- A list of figures that have associated raw data
- A description of any restrictions on data availability

The data sets generated during and/or analysed during the current study are available from the corresponding author on reasonable request. The figures 1, 2, 3 and extended data 1 to 10 have associated raw data.

Field-specific reporting

Please select the best fit for your research. If you are not sure, read the appropriate sections before making your selection.

Life sciences Behavioural & social sciences Ecological, evolutionary & environmental sciences

For a reference copy of the document with all sections, see nature.com/authors/policies/ReportingSummary-flat.pdf

Life sciences study design

All studies must disclose on these points even when the disclosure is negative.

Sample size	The sample size was chosen based on previous experience with respect to how many independent cohorts of mice and number of mice per treatment group per cohort are required to reliably detect biologically meaningful differences among groups.
Data exclusions	No data were excluded.
Replication	All mouse experiments were repeated in at least two independent cohorts and on at least three independent biological samples. All tissue culture experiments were repeated in at least three independent experiments. All attempts at replication were successful.
Randomization	The allocation of mice with the same genotype into different experimental groups was random.
Blinding	Investigators were blinded to experimental groups when assessing the maximal running distance and levels of autophagy of WT and TLR9-/mice.

Reporting for specific materials, systems and methods

Materials & experimental systems

n/a	Involved in the study
<input checked="" type="checkbox"/>	<input type="checkbox"/> Unique biological materials
<input type="checkbox"/>	<input checked="" type="checkbox"/> Antibodies
<input type="checkbox"/>	<input checked="" type="checkbox"/> Eukaryotic cell lines
<input checked="" type="checkbox"/>	<input type="checkbox"/> Palaeontology
<input type="checkbox"/>	<input checked="" type="checkbox"/> Animals and other organisms
<input checked="" type="checkbox"/>	<input type="checkbox"/> Human research participants

Methods

n/a	Involved in the study
<input checked="" type="checkbox"/>	<input type="checkbox"/> ChIP-seq
<input checked="" type="checkbox"/>	<input type="checkbox"/> Flow cytometry
<input checked="" type="checkbox"/>	<input type="checkbox"/> MRI-based neuroimaging

Antibodies

Antibodies used

For western blots, anti-beclin 1 antibody (sc11427; used at a 1:1000 dilution), anti-myc HRP antibody (sc40 HRP; used at a 1:100 dilution) and anti-β-actin HRP (sc47778 HRP; used at 1:10000 dilution) antibodies were from Santa Cruz. Anti-UVRAG antibody (#13115; used at 1:1000 dilution), anti-Vps34 antibody (#4263; used at 1:1000 dilution), anti-Atg14 antibody (#96752, to detect mouse Atg14; used at 1:1000 dilution), anti-p-AMPKα(Thr172) antibody (#2535; used at 1:2000 dilution), anti-AMPKα antibody (#2532; used at 1:1000 dilution), anti-AMPKβ1/β2 antibody (#4150; used at 1:1000 dilution), anti-p-Raptor (Ser792) antibody (#2083; used at 1:500 dilution), anti-Raptor antibody (#2280; used at 1:500 dilution), anti-TBC1D1 antibody (#66433; used at 1:1000 dilution) and anti-HA antibody (#3724, to detect Tlr9-HA in tissue lysates of Tlr9-HA KI mice; used at 1:1000 dilution) were from Cell Signaling Technology. Anti-p-ACC (Ser79) antibody (#07-303; used at 1:1000 dilution), anti-ACC antibody (#04-322; used at 1:1000 dilution) and anti-p-TBC1D1 (Ser237) antibody (#07-2268; used at 1:2000 dilution) were from Millipore. Anti-ATG14 antibody (M184-3, to detect human ATG14; used at 1:1000 dilution) was from MBL international. Anti-HA

high affinity-HRP antibody (#12013819001; used at 1:2000 dilution to detect overexpressed TLR9-HA in cells and used at 1:1000 dilution to detect Tlr9-HA after immunoprecipitation from muscle lysates of the Tlr9-HA KI mice) was from Roche. Anti-Flag M2-HRP antibody (A8592; used at 1:5000 dilution) was from Sigma. Anti-Glut4 antibody (GT41-A; used at 1:1000 dilution) was from Alpha Diagnostic International. For immunoprecipitation, anti-Beclin 1 antibody (sc48341; 10 µl per sample) was from Santa Cruz. Anti-HA high affinity antibody (#11867423001; 10 µl per sample) was from Roche. Anti-HA antibody (#3724; 6 µl per sample) was from Cell signaling Technology. Throughout the study, several lots of each antibody may have been used, and each lot behaved similarly for the experimental purposes.

Validation

All the antibodies used in the study were bought from commercial vendors and were validated by the manufacturers and/or other studies. See individual antibody's web page (link shown below) on the manufacturer's website for validation and relevant citation.

Anti-beclin 1 antibody (for western blots): <https://www.scbt.com/p/becn1-antibody-h-300>
 Anti-myc HRP antibody: <https://www.scbt.com/p/c-myc-antibody-9e10>
 Anti-β-actin HRP antibody: <https://www.scbt.com/p/beta-actin-antibody-c4>
 Anti-UVRAG antibody: <https://www.cellsignal.com/products/primary-antibodies/uvrag-d2q1z-rabbit-mab/13115>
 Anti-Vps34 antibody: <https://www.cellsignal.com/products/primary-antibodies/pi3-kinase-class-iii-d9a5-rabbit-mab/4263>
 Anti-Atg14 antibody (for detecting mouse Atg14): <https://www.cellsignal.com/products/primary-antibodies/atg14-d1a1n-rabbit-mab/96752>
 Anti-p-AMPK α (Thr172) antibody: <https://www.cellsignal.com/products/primary-antibodies/phospho-ampka-thr172-40h9-rabbit-mab/2535>
 Anti-AMPK α antibody: <https://www.cellsignal.com/products/primary-antibodies/ampka-antibody/2532>
 Anti-AMPK $\beta 1/\beta 2$ antibody: <https://www.cellsignal.com/products/primary-antibodies/ampkb1-2-57c12-rabbit-mab/4150>
 Anti-p-Raptor (Ser792) antibody: <https://www.cellsignal.com/products/primary-antibodies/phospho-raptor-ser792-antibody/2083>
 Anti-Raptor antibody: <https://www.cellsignal.com/products/primary-antibodies/raptor-24c12-rabbit-mab/2280>
 Anti-TBC1D1 antibody: <https://www.cellsignal.com/products/primary-antibodies/tbc1d1-d2y8m-rabbit-mab/66433>
 Anti-HA antibody: <https://www.cellsignal.com/products/primary-antibodies/ha-tag-c29f4-rabbit-mab/3724>
 Anti-p-ACC (Ser79) antibody: https://www.emdmillipore.com/US/en/product/Anti-phospho-Acetyl-CoA-Carboxylase-Ser79-Antibody_MM_NF-07-303
 Anti-p-TBC1D1 (Ser237) antibody: https://www.emdmillipore.com/US/en/product/Anti-phospho-TBC1D1-Antibody-Ser237_MM_NF-07-2268
 Anti-ATG14 antibody (for detecting human ATG14): <https://www.mblintl.com/products/m184-3>
 Anti-HA high affinity-HRP antibody: <https://www.sigmaldrich.com/catalog/product/roche/12013819001?lang=en®ion=US>
 Anti-Flag M2-HRP antibody: <https://www.sigmaldrich.com/catalog/product/sigma/a8592?lang=en®ion=US>
 Anti-Glut4 antibody: <https://4adi.com/4adi/anti-mouse-glucose-transp-4-glut-4-igg-1-aff-pure-11557-p.html>
 Anti-Beclin 1 antibody (for immunoprecipitation): <https://www.scbt.com/p/becn1-antibody-e-8>
 Anti-HA high affinity antibody (for immunoprecipitation): <https://www.sigmaldrich.com/catalog/product/roche/roahaha?lang=en®ion=US>

Eukaryotic cell lines

Policy information about [cell lines](#)

Cell line source(s)	Hela cells, U2OS cells, HEK293S and Phoenix cells were from ATCC
Authentication	All cell lines were obtained from and pre-authenticated by ATCC and used at very low passages (<7 passages). Hela cells was additionally authenticated by ATCC Cell Line Authentication Service using STR analysis.
Mycoplasma contamination	The cell lines were tested negative for mycoplasma contamination by PCR analysis.
Commonly misidentified lines (See ICLAC register)	No commonly misidentified cell lines were used.

Animals and other organisms

Policy information about [studies involving animals](#); [ARRIVE guidelines](#) recommended for reporting animal research

Laboratory animals	Tlr9-/ mice was described in reference 20. BCL2 AAA mice was described in reference 4 and GFP-LC3 transgenic mice was described in reference 27. All strains were rederived in the UTSW Transgenic Mouse facility on a C57BL/6J (Jackson Laboratory) background and further backcrossed to C57BL/6J for at least 10 generations. Tlr9-HA knock-in mice on a C57BL/6J background were generated as described in Methods section. Male mice with an age between 8 to 12 weeks were used in the study.
Wild animals	none
Field-collected samples	none